國 立 交 通 大 學

物 理 研 究 所

碩 士 論 文

利用NE213液態閃爍體偵檢器及氦三比例偵檢器
量測中子能譜

Neutron Detection with NE213 Liquid Scintillator and
Helium-3 Proportional Tube Detector

研 究 生： 胡貝禎

指導教授： 林貴林 教授

王正祥 教授

中 華 民 國 九 十 八 年 六 月

利用NE213液態閃爍體偵檢器及氦三比例偵檢器
量測中子能譜

Neutron Detection with NE213 Liquid Scintillator and Helium-3 Proportional Tube Detector

研 究 生 ： 胡貝禎　　　　　Student: Bei-Zhen Hu

指 導 教 授 ： 林貴林　　　　Advisor: Guey-Lin Lin

　　　　　　王正祥　　　　　　　　　Chung-Hsiang Wang

國 立 交 通 大 學

物 理 研 究 所

碩 士 論 文

A Thesis
Submitted to Institute of Physics
National Chiao Tung University
in Partial Fulfillment of the Requirements
for the Degree of
Master
in
Physics
July, 2009
Hsinchu City, Taiwan, Republic of China

中華民國九十八年六月

利用NE213液態閃爍體偵檢器及氦三比例偵檢器
量測中子能譜

學生： 胡貝禎　　　　　　　　　指 導 教 授 ： 林貴林
　　　　　　　　　　　　　　　　　　　　　　 王正祥

國立交通大學物理研究所

摘　　　要

　　中子在許多地下物理實驗站的實驗結果佔了很重要的角色。所以，研究地表下的中子是一個重要的課題。中子的研究大多是實驗與模擬並行。

　　在此，我們使用液態閃爍體偵檢器來量測中子的能譜，同時我們也使用GEANT4來模擬整個實驗。進而比較實驗以及模擬之間的關係。另外，我們也利用加速器產生質子，讓質子射入氟化鋰靶材上使他產生中子，再利用我們的探測器量測此反應所產生的中子能譜。

Neutron Detection with NE213 Liquid Scintillator and Helium-3 Proportional Tube Detector

Student: Bei-Zhen Hu   Advisor: Guey-Lin Lin
                                       Chung-Hsiang Wang

Submitted to Institute of Physics
National Chiao Tung University

ABSTRACT

Most noise of underground experiment is from muon-induced neutron process. Underground neutron fluxes are difficult to measure so most study about this are via simulation. It is important to check the normalization of the simulation by a measurement.

We use NE213 detector and Helium-3 detectors to measure the neutron spectrum. We also perform GEANT4 simulation for reconstructing the neutron energy. We use different neutron sources for the experiment. First, we hang the source on nylon and place detectors near the source for an energy measurement. We then perform GEANT4 simulation to find the response function of the NE213 detector. In this way, we can unfold the measurement result to get the real energy spectrum.

致　　謝

就像陳之藩的"謝天"文中所提：「因為需要感謝的人太多了，就感謝天吧！」

感謝天恩師德。

感謝我的家人時常給我力量。

感謝林貴林老師以及王正祥老師平日的指導。

感謝袁立基老師、牛寰老師的協助，以及Group的所有成員、清華加速器的學長們、香港的伙伴們的幫忙。

還有，感謝我身邊的所有朋友們，謝謝你們一直以來幫我加油打氣!

Contents

List of Figures

List of Tables

Chapter 1

Introduction

Daya Bay reactor antineutrino experiment [1] is one of the experiments to determine the neutrino mixing angle θ_{13}. It is expected to measure the neutrino mixing angle θ_{13} with a sensitivity of 0.01. In Daya Bay experiment, the detection is based on the inverse beta decay

$$\bar{\nu} + p \rightarrow n + e^+$$

In Daya Bay, the material of antineutrino detector is $Gd - LS^\dagger$ since the cross section for neutron capture in Gd is large. An antineutrino event contains two gamma signals, which are produced by the electron-positron annihilation and neutron capture. The time interval between those two gamma signals is about 180 microseconds. This is an important characteristic for Daya Bay experiment. So, reducing the noise of background gamma ray can improve the experiment.

In general, there are three kinds of background gamma ray. First, the decays of isotopes such as Uranium-238, Thorium-232 and Potssium-40. Second, from muon induced neutrons, which are captured by Gd. Third, from the decays of cosmogenic radio-isotopes, Li^9 and He^8. Li^9 and He^8 could emit neutrons during decay process. It is to be note that, when neutron is captured by Gadolinium, a 8-MeV gamma ray is emitted. The gamma ray energy from the isotope decay is too small comparing with the gamma ray from the neutron capture, so the most

---

†Gadolinium-Loaded Liquid Scintillators.

energetic gamma ray is from the neutron capture. In other words, gamma ray from neutrons plays an important role in the Daya Bay experiment.

The underground neutron fluxes are difficult to measure. Actually, most studies for underground neutron are via simulation. In neutron studies, there exit many kinds of neutron simulation packages and neutron measurement techniques, such as the proton recoil instruments, time-of-flight instruments, moderating detectors, proportional counters, and so on.

Since neutrons are not detected directly, there is a relation between the measured spectrum and the original spectrum. The process that transforms the measured spectrum to the original spectrum is called unfolding method. In 1981, Chen [2] used NE213 organic liquid scintillator to determine the fast neutron spectrum and apply the unfolding method with NEUTSP program to analyze the neutron spectrum. In that experiment, the neutron sources are ^{239}Pu-Be, ^{252}Cf, monoenergetic neutron from Van De Graaff accelerator and the neutrons from a water moderated reactor.

By the simulation method, one can calculate the response function, and implement, the unfolding method. One can also use the simulation toolkit to simulate the experiments and compare with measurements. In 1997, Martin Karlsson [3] used NE213 organic liquid scintillator to detect neutron by the method of time-of-flight with ^{252}Cf source. He then compared the result with Stanton code calculations and the GEANT simulation.

For the simulation, different simulation toolkits give rise to different results. In 2007, Yeh [4] compared the simulation results of neutron propagations given by FLUKA, GEANT4 and MCNP. It was pointed out that, at the low energy (E<100 MeV), the result of GEANT4 simulation was similar to that by FLUKA, and at the high energy range (E>100 MeV), the GEANT4 result was close to that by MCNP. Therefore, it is important to check the normalization of the simulation by a measurement.

In this thesis, we use NE213 organic liquid scintillator and Helium-3 proportional tube to detect neutron. We also use GEANT4 to simulate the experiment

and compare the simulation result with the measurements. We used two kinds of neutron source. One is a mixture of ^{238}Pu and ^{13}C. Neutrons are produced by two steps, which will be discussed in Chapter 1. We also use the accelerator to produce proton and have the proton impact on the ^{7}Li target. This procedure produces monoenergetic neutron, this is the second type of neutron source. The details are discussed in Chapter 5. The DAQ (Data Acquisition) system for the detector is the standard NIM (Nuclear Instrumentation Module) system. We use pulse shape method to measure the neutron spectrum. The details are discussed in Chapter 3.

Chapter 2

The Principle of Neutron Detection

2.1 Interactions between neutron and matter

The techniques of particle detection are based on the interaction between charge particle and the matter of detectors. Since neutrons are neutral particles, the methods for neutron detections are not direct. Detector detects the charged particles or radiations that are produced from neutrons interacting with the nucleus. There are many types of neutron detection methods, such as scattering reaction method, nucleus reaction methods, fission method, and foil activation method. Table 2.1 shows the nucleus reaction method.

2.1.1 Neutron elastic scattering

When a neutron collides with a nucleus, the recoil nucleus gets the part of kinetic energy from neutron and ionizes the matter of detector. Sebsequently, the molecules in the detector are excited by those ions.

We can consider two frames, center-of-mass frame and lab frame, for the collisions happening in the organic liquid scintilltor. These are shown in Fig. 2.1.

Reaction Functions	Name
$n + {}^A_Z X \rightarrow {}^A_Z X + n$	Scattering/ Recoil nucleus
$n + {}^A_Z X \rightarrow {}^A_{Z-1} Y + p$	(n, p) reaction
$n + {}^A_Z X \rightarrow {}^{A-3}_{Z-1} Y + He$	(n, α) reaction
$n + {}^A_Z X \rightarrow {}^A_{Z+1} Y + 2n$	(n, γ) reaction/ neutron capture
$n + {}^A_Z X \rightarrow {}^{A_1}_{Z_1} Y_1 + {}^{A_2}_{Z_2} Y_2 + n + n + \ldots$	fission

Table 2.1: The list of neutron-nucleus reaction [8].
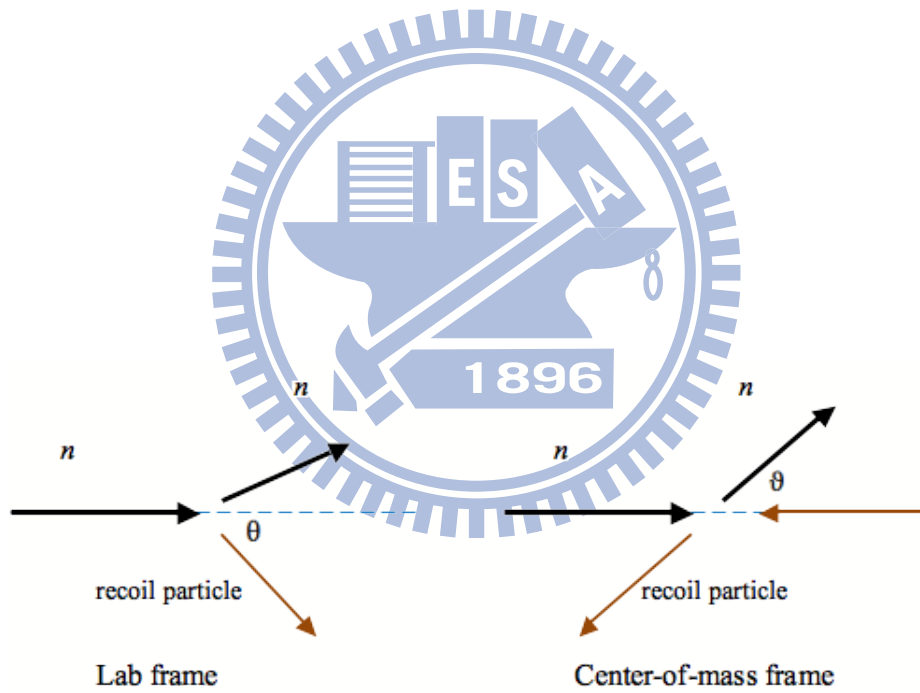
Figure 2.1: Neutron elastic scattering in lab frame and center-of-mass frame.

The energy relation between the recoil nucleus and neutron is:

$$E_r = \left(\frac{4A}{(1+A)^2} \right) \cos^2 \theta \cdot E_n \qquad (2.1)$$

And the relation between these two frames is

$$\cos \theta = \sqrt{\frac{1 - \cos \vartheta}{2}}, \qquad (2.2)$$

where A is mass of target nucleus, E_n is neutron incident kinetic energy, E_r is recoil nucleus kinetic energy, θ is the angle of nucleus recoil in the lab frame, and ϑ is the angle of scattering neutron in the center-of-mass frame [5].

2.1.2 Nucleus reaction

As shown in Table 2.1, when neutron collides with nucleus, the process causes the nucleus to change atomic number (Z) or atomic mass (A) and produce charged particles. Some neutron detection methods are based on this principle. Following are the most popular reactions for neutron detection.

The $^{10}B(n, \alpha)$ reaction

$$^{10}_{5}B + ^{1}_{0}n \rightarrow ^{7}_{3}Li^* + ^{4}_{2}He \qquad Q - value = 2.310 \text{ MeV}(94\%) \qquad (2.3)$$

$$^{10}_{5}B + ^{1}_{0}n \rightarrow ^{7}_{3}Li + ^{4}_{2}He \qquad Q - value = 2.792 \text{ MeV}(6\%) \qquad (2.4)$$

$$^{7}_{3}Li^* \rightarrow \gamma + ^{7}_{3}Li \qquad Q - value = 0.478 \text{ MeV} \qquad (2.5)$$
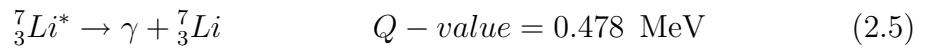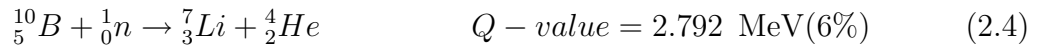
When neutron collides with ^{10}B, the probability of the production to be on the excited state, $^{7}_{3}Li^*$ is 94% and the probability is 6 % for the production to be on the ground state $^{7}_{3}Li$. When the excited ^{7}Li de-excites to the ground state, it liberates γ-ray with an energy of 0.478 MeV.

The $^6Li(n, \alpha)$ reaction

$$^6_3Li + ^1_0n \rightarrow ^3_1H + ^4_2He \qquad\qquad Q - value = 4.78 \text{ MeV} \qquad (2.6)$$
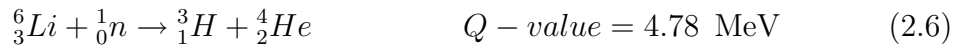
This is another (n, α) reaction and the targets are ^6Li. Since the Q-value of this reaction is high, it is easy to discriminate the signal from gamma ray.

The $^3He(n, p)$ reaction

$$^3_2He + ^1_0n \rightarrow ^1_1H + ^3_1H \qquad\qquad Q - value = 0.764 \text{ MeV} \qquad (2.7)$$
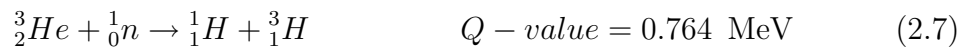
As shown in Eq. (2.7), neutron interacts with helium-3 and produces triton and proton. Since the reaction Q-value is very low, it is not easy to discriminate the signals from gamma ray.

2.1.3 Neutron-Induced Fission Reactions

Neutron collides with heavy nucleus and cause nucleus fission. The method of detecting the fragments, which are the products of nucleus fission, is called fission method. The ^{235}U, ^{239}Pu, and ^{233}U are used as the fission materials. The energy liberated during nucleus fission is about 200 MeV. About 165 MeV is taken away by two fragments. Since the energy is very large, the γ-ray does not affect the measurement.

2.1.4 Foil Activation

Neutron interacts with atomic nucleus and produces complex nucleus. In general, the complex nucleus is at excited state so it will emit gamma and beta radiations. By detecting the intensity of these radiations, one can calculate the intensity of the neutron.

2.2 The structure of detector

In this experiment, the detectors we choose are organic liquid scintillator and ^3He proportional gas tube and they are based on the neutron elastic scattering and (n, p) reaction respectively. So, we need to know the structure of these detectors.

2.2.1 Organic Liquid Scintillator Mechanism

Overall, the fluorescence process in the organics is due to the free electron transitions between the energy levels of the molecule. The energy level of the molecule is shown in Fig. 2.2, and it is known as the π-electron structure. As shown in the picture, there are singlet states and triplet states; S_x labels the former and T_x labels the latter, and S_{xy} labels the vibration states. As one can see, the label S_{00} is the ground state of the molecule.
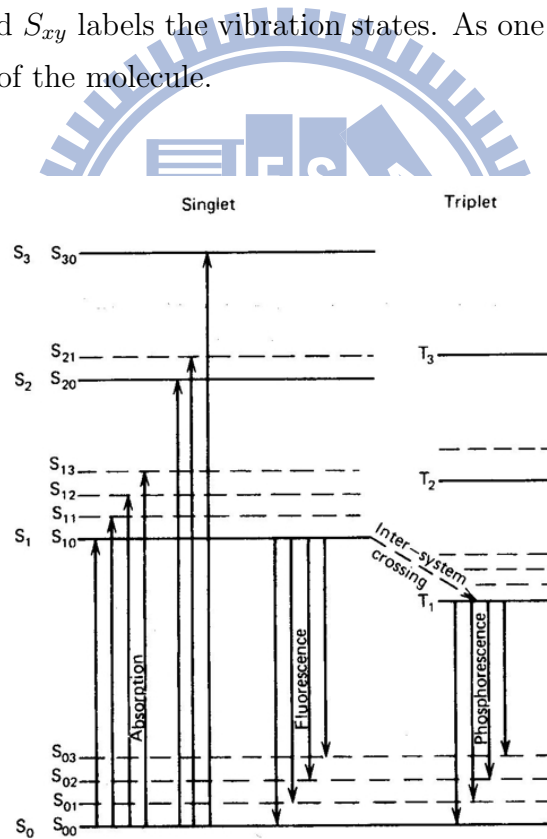
Figure 2.2: π-electron energy level. From J. B. Birks [9].

The charged particles pass through the detector and lose energies. The free electrons in the molecule absorb the energy and jump to the higher energy levels; these states are the so-called excited states. By the internal conversion process, the excited state immediately becomes de-excited to S_1 state or its vibration state (such as S_{11}, S_{12}, etc.) without emitting radiation. Finally, the S_{10} state transits to one of the vibration states of the ground state, S_{0y}. This process emits the scintillation light. Another process proceeds as the excited state goes through intersystem crossing to the triplet state T_1 then transits to S_0. This process also emits the light called phosphorescence. While at the T_1 state, the molecule may go back to S_{10} state and then decay to S_{0y} state. The scintillation light from this process is called delayed fluorescence.

NE213 Scintillator

The NE213[†] scintillator is a kind of organic liquid scintillators. It consists of xylene, activators, and naphthalene. The density of NE213 is 870 kg/m^3, and the radio of H to C is 1.213 [6][8]. There is another scintillator named BC01A which has the same content as NE213. They are widely used for the fast neutron detection since their good pulse discrimination.

2.2.2   Gas-Filled Detector

The earlier detector used to detect radiation is gas-filled detector. This kind of detector includes two parts, electrodes and gas. The role of the electrodes is to provide the electric field. The principle of gas-filled detectors is based on ionization and excitation of gas molecules. When the radiation or charged particles pass through the gas tube, the electron-ion pairs are produced. Due to the electric field, the electron and charged ions will move to anode and dynode respectively.

[†]A type of NE series of organic scintillators is manufactured by Nuclear Enterprises, Winnipeg, Ontario, Canada.

The gas-filled detector can be divided to three categories (ion chambers, proportional counters, and Geiger tubes) by using different operation high voltage. The relation between pulse amplitude output from the detector and the applied voltage is shown in Fig. 2.3. At the very low voltage region, electric field in the tube is not strong, and electron and charged ions are at slow speeds. Hence, there is a very large chance for charged particles to recombine. In the second region, the recombination rate is zero, and there is no charge multiplication. The ionization chambers operate in this region. As the voltage increases, the charge multiplication effect becomes non-negligible, and there is a range that the collected charge is proportional to the number of the electron-ion pairs produced by the incident radiation. We call this region proportional region and the proportional tube is operating in this region. As the voltage further increases, the charge multiplication effect becomes non-linear. If the multiplication effect become serious, called avalanche, the light output from the detector is incapable of distinguishing the energy of incident radiation. This region is called the Geiger-Mueller region.
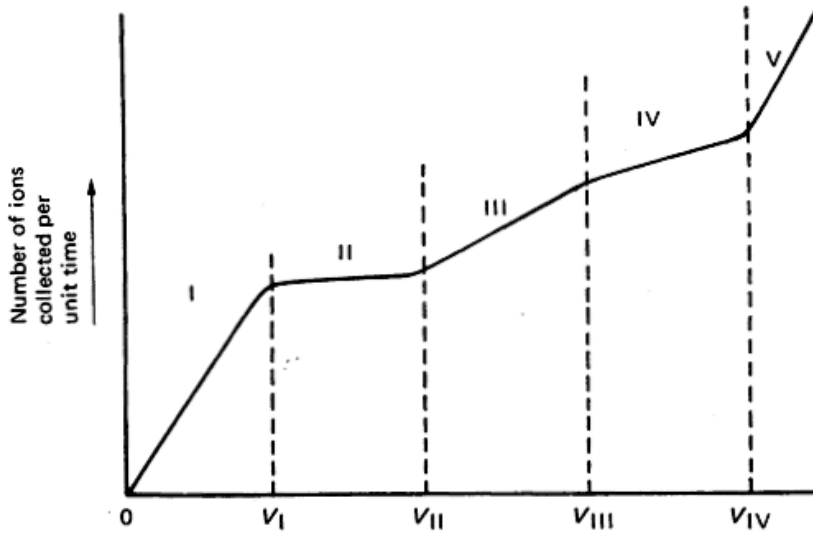
Figure 2.3: The relation between high voltage and pulse amplitude. From N. Tsoulfanidis [8].

^3He **Proportional Tube**

The proportional tube filled with ^3He gas is widely used for the neutron detection, including the detection of thermal neutron and the fast neutron.

When the neutron interacts with ^3He and produces triton and proton, the reaction Q-value is shared by proton and triton which then deposit the energy by ionizing the gas or exciting the atom in the tube.

The proportional tube we used is in a cylindrical shape and made of aluminum. The length is 11.5 inch and the diameter is 2.0 inch. The gas pressure inside the cylinder is 3040 torr.

2.3 Neutron Source

The neutron source is a mixture of ^{238}Pu and ^{13}C. Neutrons are produced through a two-step reaction:

$$^{238}_{94}Pu \rightarrow ^{234}_{92}U + ^4_2He \qquad Q-value = 5.60181 \text{ MeV} \qquad (2.8)$$

$$^4_2He + ^{13}_6C \rightarrow ^1_0n + ^{16}_8O \qquad Q-value = 2.21423 \text{ MeV} \qquad (2.9)$$

$$^{17}_8O^* \rightarrow \gamma + ^{17}_8O \qquad Q-value = 6.3310 \text{ MeV} \qquad (2.10)$$
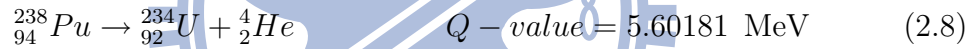
Plutonium-238 is a kind of radioactive isotope of Plutonium. Its decay produces Uranium-234 and an alpha with the Q-value 5.60181 MeV. The alpha particle acquires a kinetic energy T=5.50025 MeV. We can estimate the neutron energy by the energy conservation. The neutron energy is between 4.7536 MeV and 7.478 MeV.

Chapter 3

Experiment Details

3.1 Experimental Setup

The experiment took place at the lab of Biomedical Engineering and Environmental Science Department at NTHU. The electronics setup is shown in Fig. 3.1 and Fig. 3.2, and the detector setup is shown in Fig. 3.3. As one can see, there are two detecting systems in this experiment, NE213 scintillator and ^3He proportional tube. The neutron source was hanged for reducing the neutron scattering. The distance between neutron source and detector is 20 cm.
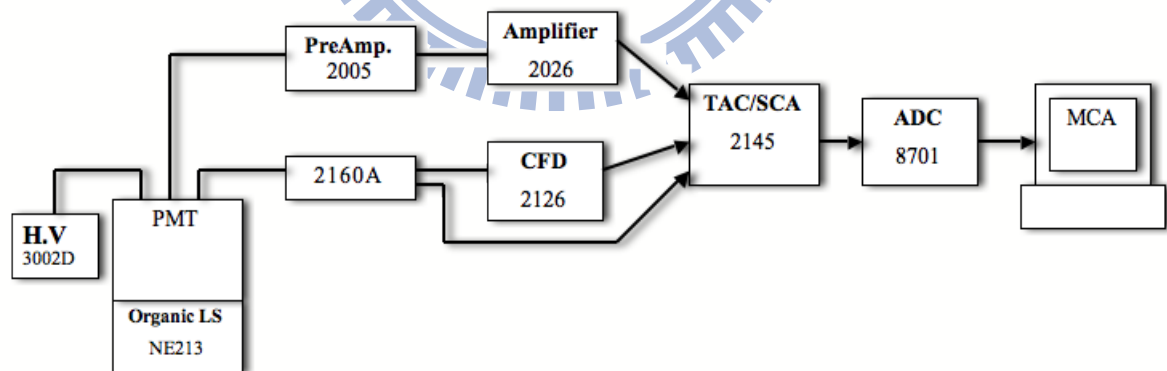
Figure 3.1: The electronics setup: NE213 liquid scintillatior system.
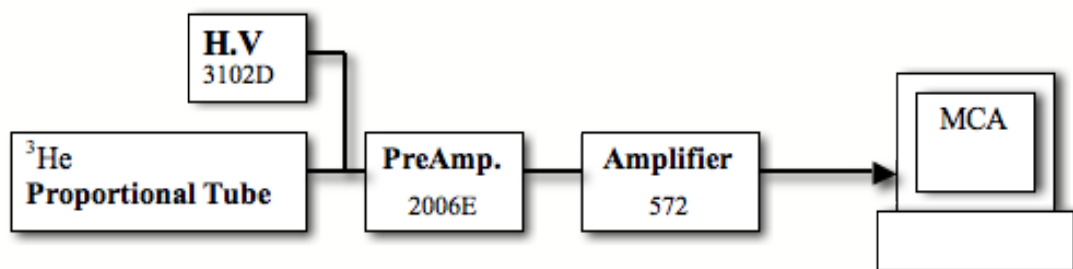
Figure 3.2: The electronics setup: ^3He proportional tube system.
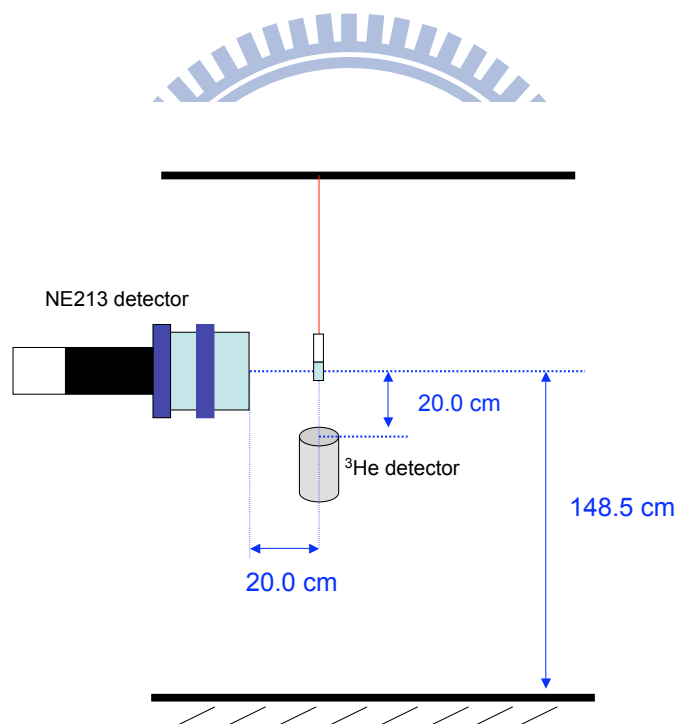
Figure 3.3: The experiment setup.

The keywords of the electronic setup system:

(a) NE213 liquid scintillatior system

1. H.V 3002D ：High voltage power supply, Module 3002D, CANBERRA.

2. PreAmp. ：Preamplifier, Module 2005, CANBERRA.

3. Amplifier 2026： Amplifier, Module 2026, CANBERRA.

4. 2160A：Pulse Shape Discriminator, Module 2160A, CANBERRA.

5. CFD 2126：Constant Fraction Discriminator, Module 2126, CANBERRA.

6. TAC/SCA 2145：Time-Amplitude-Converter/ Signal-Channel-Analyzer, Module 2145, CANBERRA.

7. ADC 8701：Analog-to-Digital Converter, Module 8701, CANBERRA.

8. MCA：Multiple Channel Analyzer

(b) ^3He proportional tube system

1. H.V 3102D ：High voltage power supply, Module 3002D, CANBERRA.

2. PreAmp. ：Preamplifier, Module 2006E, CANBERRA.

3. Amplifier 572： Amplifier, Module 572, ORTEC.

4. MCA：Multiple Channel Analyzer

The scintillator is in contacts with PMT (Photo Multiplier Tube) and the high voltage applied to the PMT was -2000 V. The signal output from PMT can be divided into two parts, one is for the energy spectrum, and another is for the pulse shape discrimination. The former signal goes through the preamplifier, the amplifier, finally, to the ADC (Analog-to-Digital Converter). The latter one is an anode output. The signal was divided into two; one is fed into the constant fraction discriminator (Module 2126), another one is fed into pulse shape discriminator (Module 2160A). The modules will register the signals and then output step signals. These step signals were fed into TDC (Time-to-Digital Converter). The signal from Module 2126 is the start signal, and the signal from Module 2160A

is the stop signal. We can select any time window we want, and then the TDC module will output a gate signal. Finally, we fed this gate signal into ADC module to perform coincident with the signal from amplitude. After coincident method, the signal will be sent to MCA.

For ^3He proportional tube detection system, the high voltage supply to the anode of the proportional tube was +1300 V. There is no need to do the pulse shape discrimination, since the reaction in the tube is mainly depending on (n, p) reaction. The energies, deposited by proton and triton are proportional to the pulse height. Signals passed through the preamplifier first, and were then fed into the amplifier. After that, signals were sent to MCA.

3.1.1 Preamplifier

The purposes for using preamplifier is for a good coupling between the detector and the counting system and a minimization of the noise. There are three type of preamplifier, charge-sensitive, current-sensitive, and voltage-sensitive.

For the NE213 detecting system, the preamplifier is Model 2005 which is a charge-sensitive preamplifier, the functional schematic is shown in Fig. 3.4 There are three parts in the Model 2005, integrator, P/Z (pole/zero), and buffer. In the integrator circuit, the feedback capacitor of the preamplifier collects the charges from the detector, the output voltage is proportional to the charge from the detector since V_0=Q/C. The P/Z circuit is for optimizing the signal performance. The differentiator is made of a capacitor of the P/Z circuit and the resistor. It provides the 50 μs tail pulse. The capability of the buffer circuit is to avoid the pulse degradation. The features of this preamplifier are low noise, high charge rate capacity (up to 9 μC/s), and fast risetime (less than 15 ns).

For the He^3 detector, the preamplifier is Model 2006. This preamplifier is also the charge-sensitive preamplifier which is shown in Fig. 3.5. But this model is for the proportional counter.
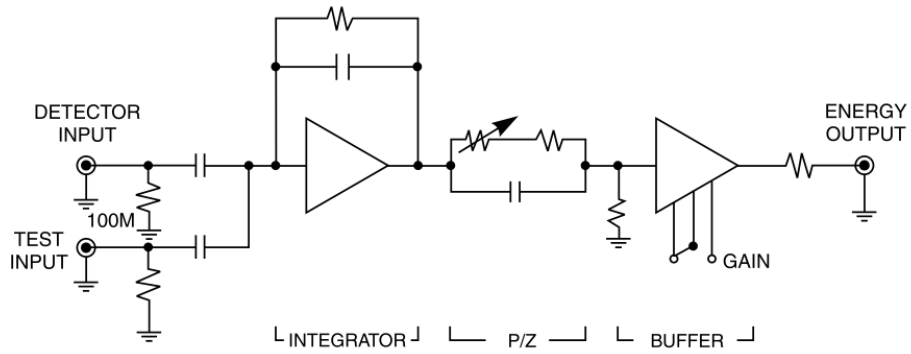
15

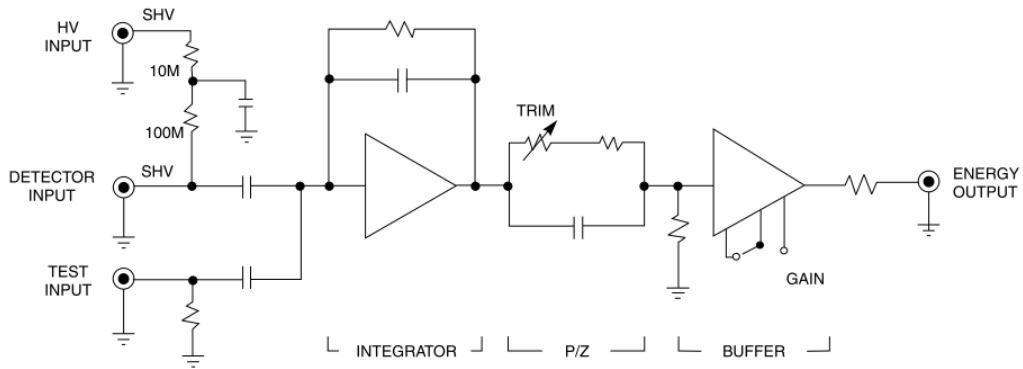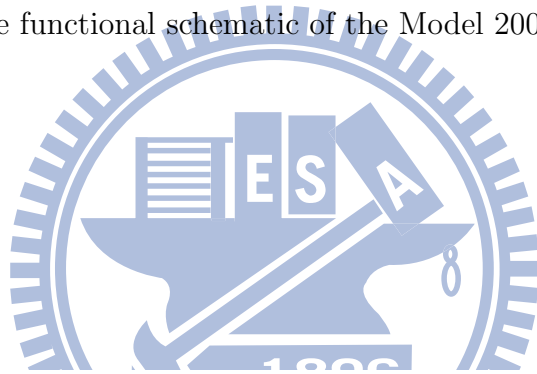Figure 3.4: The functional schematic of the Model 2005 preamplifier.

Figure 3.5: The functional schematic of the Model 2006 preamplifier.

16

3.1.2 Amplifier

The signals output from the preamplifier can not be sent too far away since they are just a few millivolts. In general, the amplifier is used to amplify and shape the signal. It can avoid the signal pile-up and improve the signal-to-noise ratio.

In the NE213 detecting system, we use the Model 2026 Spectroscopy Amplifier. There are three pulse shape modes, Gaussian, Triangular and bipolar. For shaping time selection, there are six-position switch we can select. They are 0.5, 1, 2, 4, 6, and 12 μs. The gain range is variable from 2.5 to 1500 with the eight-position switch, the coarse gain ($\times 5$, $\times 10$, $\times 20$, $\times 50$, $\times 100$, $\times 200$, $\times 500$, and $\times 1000$), and ten-turn potentiometer, the fine gain which is variable from $\times 0.5$ to $\times 1.5$. In the experiment, we selected the Gaussian mode and set the shaping time at 1.0 μs. The gain is 100×7.55 (coarse gain $\times$ fine gain).

For the He^3 proportional tube, we use the ORTEC Model 572 Amplifier to shape the signal. The pulse shape output from the amplifier is semi-Gaussian. There are two shaping mode to choice, unipolar and bipolar. The gain range is variable from 1 to 1500 with the six-position switch, coarse gain ($\times 20$, $\times 50$, $\times 100$, $\times 200$, $\times 500$, and $\times 1000$), and ten-turn potentiometer, the variable gain from $\times 0.5$ to $\times 1.5$. There are also six position, 0.5, 1, 2, 3, 6, and 10 μs, which we can choose for shaping the time.

3.1.3 Discriminator

The discriminator is used to determine the signals that we want. In general, we use some conditions, called threshold or discrimination level, to determine the signals. If the amplitude of an input signal is larger than the threshold value, the discriminator produces a logic signal, and vice versa. In this experiment, we use two discriminators, the Model 2126 and the Model 2160A, to find the neutron signals.

The Model 2126 accepts the negative signals and the output signal are both positive and negative. The count rate is 200 MHz. There are three timing modes,

constant fraction function, leading-edge, and slow rise time rejection. We can select one of them on the front panel. In addition, the threshold level is also selected on the front panel, it is the ten-turn potentiometer and the range of the threshold level are between -5 mV to -1 V. In the experiment, we selected the leading edge timing method and the threshold level is set at the scale 0.3.

The Model 2160A also accepts the negative signals and the output signal are both positive and negative. The timing method of the Model 2160A discriminator used is zero-crossing. Since this module is used under the zero-crossing method, it does not need to set the threshold level.

3.1.4 Time to Amplitude Converter and Single Channel Analyzer

The Model 2145 includes two parts, time-to-amplitude converter (TAC) and single-channel analyzer (SCA). The purpose of this module is to separate different particles, such as neutron and gamma.

The TAC part is used to analyze the time constant of different particles. The two signals are fed into this module, and then TAC circuit part generates a signal with an amplitude proportional to the time interval. For the same particle, the time interval of the signals are almost close, that is the amplitude of the TAC output is almost the same, which is called the time constant. The usable time range is between 5 ns and 1 ms.

The other part of the Model 2145 is SCA. It is also a discriminator, which requires two conditions to determine the signals.[†] It produces a logic signal only when the amplitude of an input signal is larger than the lower level threshold and smaller than the upper level threshold.

After the signal passes through the TAC part, it flows to the SCA part. The

---

[†]The discriminator we have discussed in last subsection is also called integral discriminator, comparing to this, the single channel analyzer is called differential discriminator. The former uses one condition to determine the signals. The later one uses two conditions, lower-level discriminator (LLD) and upper-level discriminator (ULD), to determine the signals.

module produces the logic signal when the amplitude of the TAC signal locates in the interval of the threshold levels. This signals are fed to the ADC module and coincident with the signal from the amplifier. The threshold levels can be select at the front panel controls.

3.1.5   Analog to Digital Converter

The analog-to-digital converter (ADC) is used to convert a continuous signals to discrete signals. After a signal passes through the ADC, the ADC produces a number that is proportional to the pulse height of the signal. In general, the number is called channel number.

The Model 8701 is Wilkinson type analog-to-digital converter. This ADC is used at the peak detection method. The clock of this model is 100 MHz and the resolution is up to 8192 channels. There are two conversion modes, Pulse Height Analysis(PHA) and Sampled Voltage Analysis(SVA). The former method is usually used. For peak detection, there are also two modes, automatic and delayed. In the automatic mode, when the signal above the threshold, the linear gate opens. When the amplitude of the signal is below 90% of its pules height, the linear gate closes. However, when the wide pulses come, the automatic detection may contain uncertainty. Therefore, the delayed mode could be used for solving this problem. In this mode, the linear gate closes at the end of the selected delay time.

In this experiment, we set the resolution to 256 channels. In addition, we use automatic peak detection and PHA mode conversion.

3.1.6   Multiple Channel Analyzer

The instrument used to record the number is called the Multiple Channel Analyzer. In the experiment, there are two different MCA software for two systems. One is called System 100 (S100); the other is called ACCUSPEC. The former is for NE213 detection system and it operates under the windows 3.0 OS. The later one

is for ^3He proportional tube, it operates under the dos OS.

3.2   Pulse Shape Discrimination

As mentioned before, the particles pass through the detector will excite the organic liquid scintillator. There are three modes of de-excitation. Two of these emit scintillation light which is the fluorescence and phosphorescence respectively. The former is the fast light and the latter is the slow one. The time of light emission affects the shape of the light output, so does the stopping powers (dE/dx) [6]. The light output for different particles are shown in Fig. 3.6. We use this characteristic to separate neutron from gamma ray. This method is called Pulse Shape Discrimination. In general, it takes two steps to implement. Fist, discriminate the arrival time of the pulse. Second, integrating the charge over two time periods.
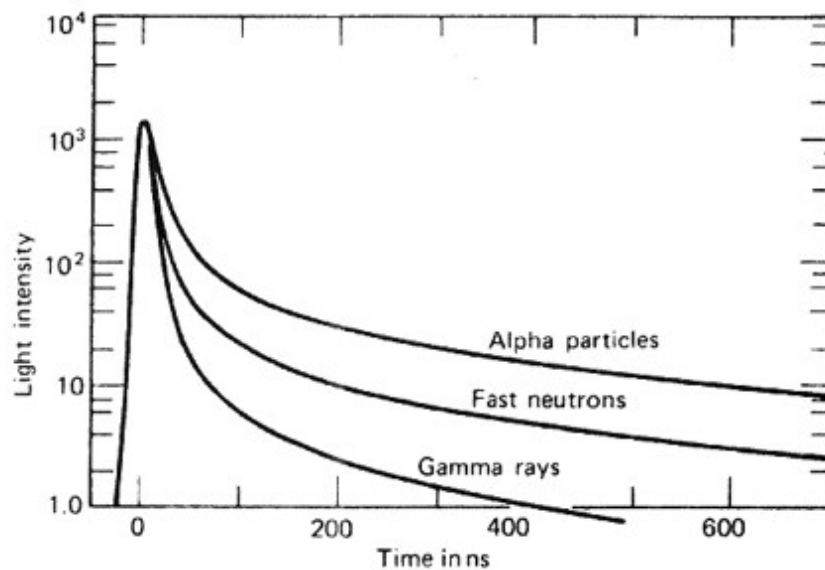

Figure 3.6: The time dependence of scintillation pulses in stilbene. From Bollinger and Thomas [7].

The method to determinate the arrival time of a pulse is called timing. This

is done in the Module 2126 and the Module 2160A.

In general, there are three methods, the leading-edge timing method, the constant-fraction timing method, and the zero-crossing timing method. The Module 2126 is Constant Fraction Discriminator module. Actually, there are three modes, constant fraction, slow risetime rejection, and leading edge, in the module. We use leading edge mode to determine the arrival time of the pulse. The method used by Module 2160A is zero-crossing method.

The signal from anode output is divided into two. One is sent to the Module 2126. The module will output a gate signal when the pulse front crosses the threshold level. The other signal is sent to the Module 2160A. In this module, the signal become a bipolar signal. As shown in Fig. 3.7, the two signals can be separated by the zero-crossing points. The module 2160A is triggered by the zero-crossing point and output a gate signal.
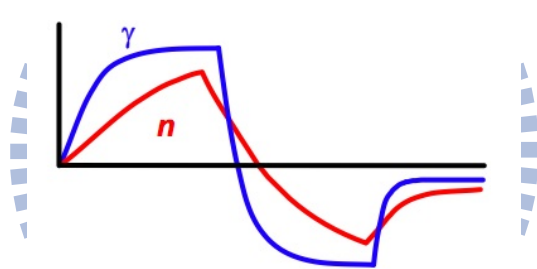
Figure 3.7: The bipolar signals.

These two gate signals are fed to the time-to-amplitude converter (TAC). When the faster signal arrives at the TAC module, the module starts to integrate. When the slower one arrives, the module stops to integrate and outputs a signal. The amplitude of a signal output depends on the time interval between start and stop signals. The diagram of pulse shape discrimination is shown in Fig. 3.8. For the same particle, the time interval is almost constant. We call such an interval the time constant of the particle. By using MCA we can get the "time spectrum" of the events that are from the detector, such as that shown in Fig. 3.9.

Fig. 3.10 shows the start and stop signal output from discriminators, taken by

Figure 3.8: The diagram of pulse shape discrimination.

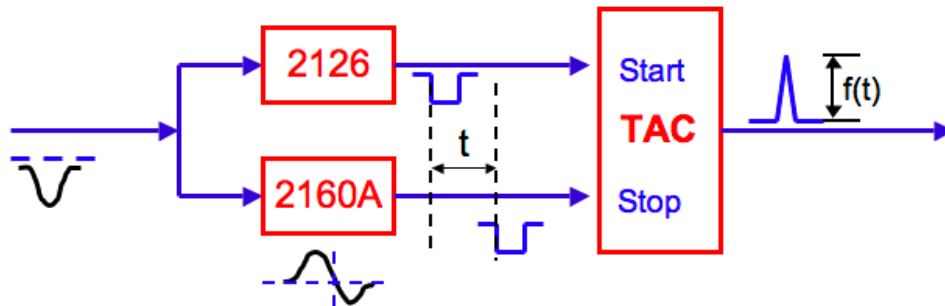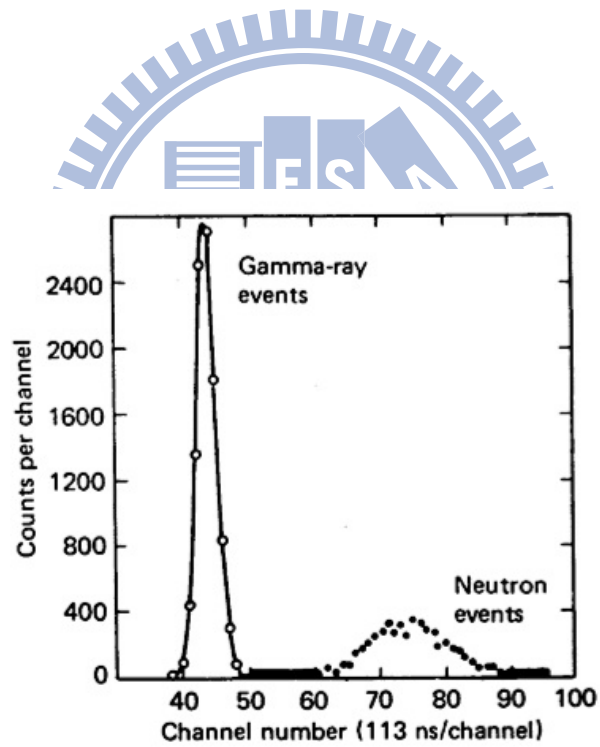Figure 3.9: After time-to-amplitude converter, gamma and neutron signals recorded by MCA. From N. Tsoulfanidis [8].

the scope. The upper signal in the picture is the start signal. The interval for two signals is 172.0 nano seconds.
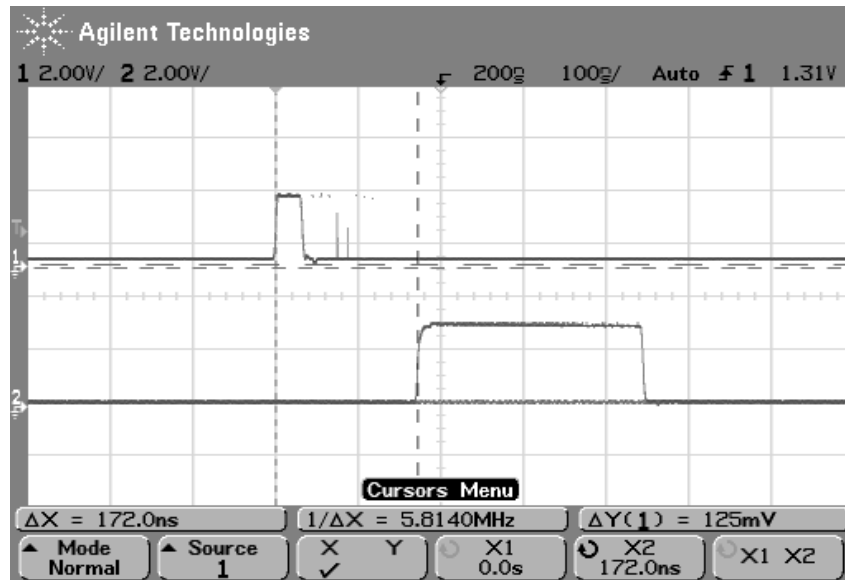
Figure 3.10: The start and stop signals captured by scope. The upper one is the start signal; and the lower one is the stop signal.

3.3 MCA Channel Calibration

Before the spectrum measurement, it is important to perform the MCA channel calibration. We need to ensure the linear relation between signal pulse height and channel numbers and check if the line passes through the zero point.

We use a pulser to generate a pulse which goes through the amplifier and is then fed into the MCA software, the diagram of the calibration circuit is shown in Fig. 3.11. Using the pulse with different height and record the channel number on MCA, we plot the relation between pulse height and channel number.

Figure 3.11: The diagram of MCA calibration circuit.

3.4   Gamma Source Calibration

When the charge particles pass through the detector and loss their energy, the electron energy levels of the molecule become excited state. After the energy level becomes de-excited state, there are scintillation light emitted. The energy of the scintillation l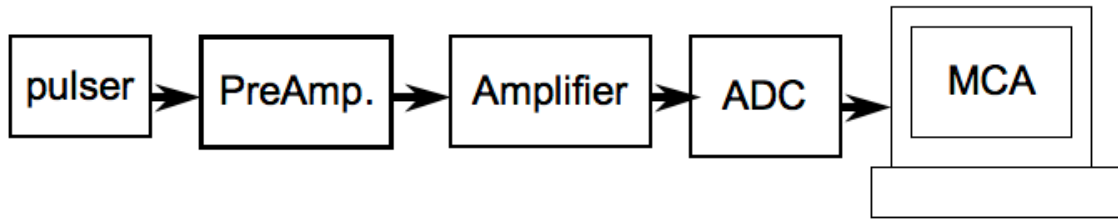ight is related to the energy of the excited electron. In addition, when particles pass through the detector, how much energies could be converted to the scintillation light depends on the particle type and its energy. There are contain relationships between the light output, particles, and the particle energies. As shown in Fig. 3.12, for NE213 organic liquid scintillators, there exist a nonlinear relation between light output and energies for heavy charged particles, such as protons and alpha particles. However this relation is linear for the electron at low energies. Therefore, for determining the proton energy scale, we first need to find out the relationship between the MCA channels and the electron energies from the detector. We then transform the electron energy scale to the proton energy scale.

Since the NE213 scintillators are sensitive to gamma ray, we used three kinds of gamma source, which are shown in Table 3.1, to calibrate this system. The interactions between gamma ray and matter are photoelectric effect, Compton scattering, and pair production [5]. The relative importance of these three effects is related with different materials and gamma ray energies. As one can see, in Fig. 3.13, the materials of absorber in the experiment are Hydrogen and Carbon, so the number of Z of absorber are 1 and 12. For the calibration gamma sources,

24
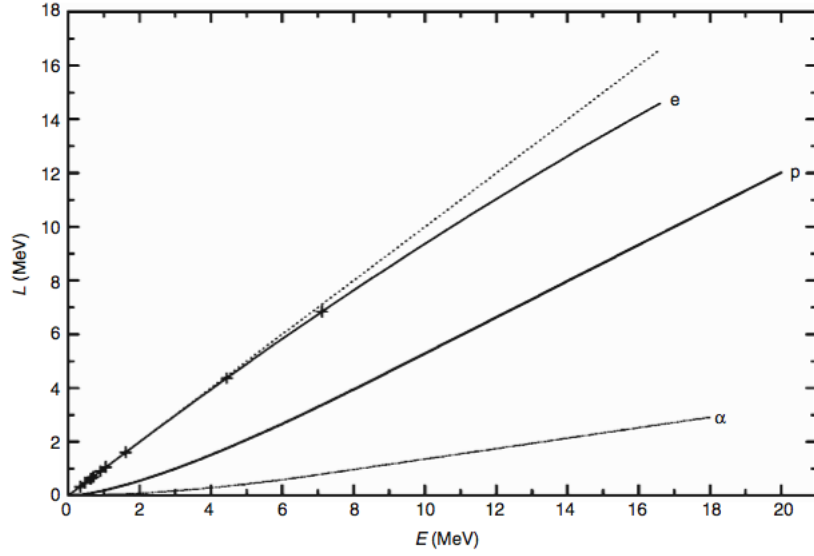
Figure 3.12: The light output for three types of gamma ray interaction. From Klein and Neumann [10].
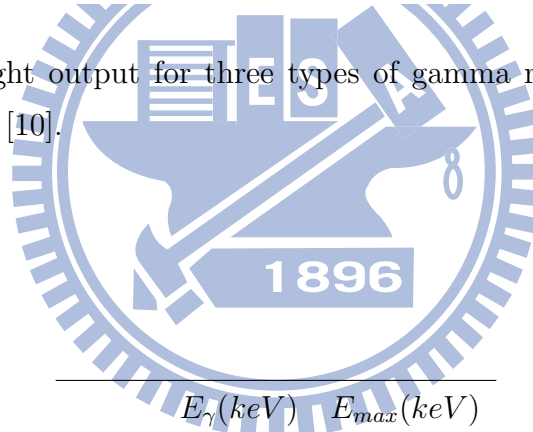
	$E_\gamma(keV)$	$E_{max}(keV)$
^{22}Na	511	340.667
	1274.542	1061.71
^{137}Cs	661.660	477.336
^{54}Mn	834.830	639.202

Table 3.1: Gamma sources. E_{max} is the maximum electron energy resulted from Compton scattering.

the energies of them are between 0.5 and 1 MeV. Therefore, the locations of these cases are at Compton effect dominant section. That is, the gamma detection using the NE213 scintillators is mainly through the Compton scattering.

Figure 3.13: Light output function $L(E)$ for electrons, protons and alpha particles, which are detected by 2×2 inch NE213 detector. From R. D. Evans [11].

The result of a Compton scattering interaction is a recoiled electron and scattered photon. The recoiled electron brings a part of energy of incident photon and the energy is related to the scattering angle. The energy of recoiled electron is given by
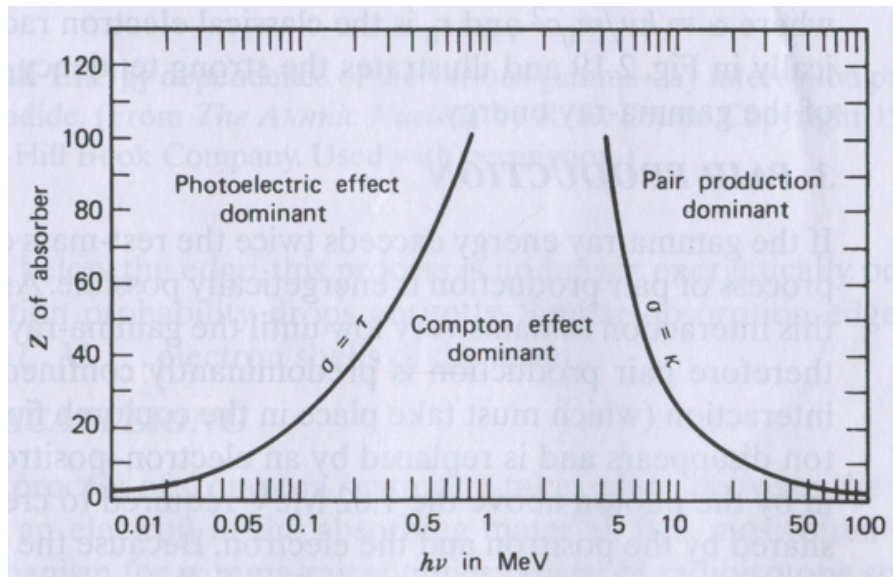
$$E_{e^-} = \frac{(E_\gamma/m_0 c^2)(1 - \cos\theta)}{1 + (E_\gamma/m_0 c^2)(1 - \cos\theta)} E_\gamma, \tag{3.1}$$

where E_γ is incident gamma ray energy, θ is the scattering angle that is between the direction of the incident gamma ray and the direction of the scattering gamma ray, c is the speed of light [5].

The scattering angle is between 0 and 180 degrees. In general, the electron energy distribution is like the picture shown in Fig. 3.14. When the scattering angle equals to 180 degree, there is a maximum value of electron energy. As one

can see, there is a cut off in the Fig. 3.14, called Compton edge. The maximum
energy is given by

$$E_{max} = \frac{2E_\gamma/m_0c^2}{1 + (2E_\gamma/m_0c^2)} \; E_\gamma \tag{3.2}$$
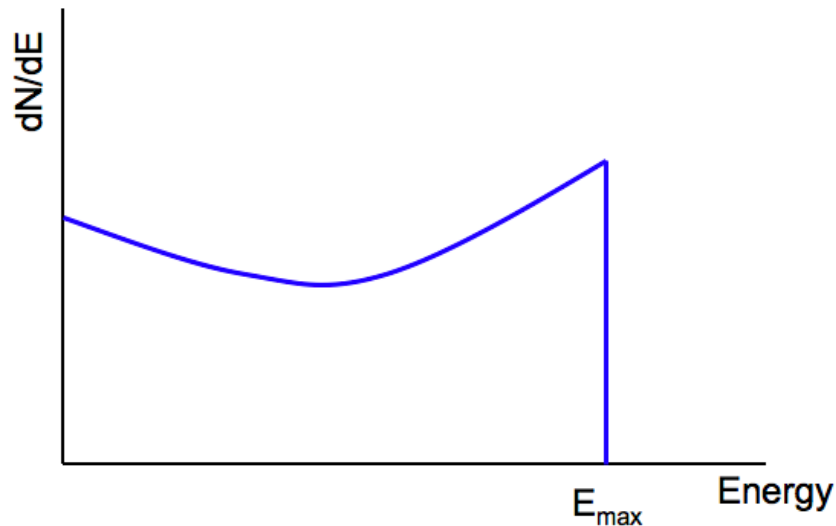

Figure 3.14: The general spectrum of scattering electrions.

We find the correspondence between the channel number and the electron en-
ergy at Compton edge. To find the Compton edge, we smoothed the measured
data and differentiated these data points. We can then determine the relation
between the MCA channel and the electron energy by data fittings. The results
are shown in Chapter 6.

Chapter 4

Simulation

4.1 A Brief Introduction To GEANT4 Simulation

GEANT4 is a simulation toolkit using Monte Carlo methods and written in the C++ language. It can be used for simulating the process of particles through matter and it has standard tools to help users to input information[13]. So, we do not need to write all the program by ourself, just modify some important classes. These classes are:

Detector Construction class

We create the detector in this class. For creating the detector, we need to describe its materials, shape, and position. First, we have to declare the elements of materials. Therefore, we can include the elements into the materials we created. After that, we can create the detector or targets.

In GEANT4, a detector is made of some volumes. For creating volumes, we need to describe their shape and physical characteristics, such as the materials, position and geometry. There are many basic geometry elements to choose, such as box, cylinder, trapezoid, tube, cone, and so on. The Fig. 4.1 and Fig. 4.2 show

the fragments of the code.

```
//Elements
  a = 1.0079*g/mole;
  G4Element* elH = new  G4Element(name="Hydrogen", symbol="H", z=1, a);
  a = 12.0107*g/mole;
  G4Element* elC = new  G4Element(name="Carbon",   symbol="C", z=6, a);
  a = 14.0067*g/mole;
  G4Element* elN = new  G4Element(name="Nitrogen", symbol="N", z=7, a);
  a = 15.9994*g/mole;
  G4Element* elO = new  G4Element(name="Oxygen",   symbol="O", z=8, a);

  //Air
  density = 1.29*mg/cm3;
  G4double temperature =293.15*kelvin;
  G4double pressure=1.*atmosphere;

  G4Material* Air = new G4Material(name="Air", density, nel=2,kStateGas,temperature, pressure);
  Air->AddElement(elN,70*perCent);
  Air->AddElement(elO,30*perCent);

  //NE213
  density = 0.874*g/cm3;
  G4Material* NE213 = new G4Material(name="NE213", density, nel=2);
  NE213->AddElement(elH,0.54812);
  NE213->AddElement(elC,0.45188);

  //Acrylic  (CH2=C(CH3)CO2CH3)
  density = 1.18*g/cm3;
  G4Material* Acrylic = new G4Material(name="Acrylic", density, nel=3);
  Acrylic->AddElement(elC, 0.59984);
  Acrylic->AddElement(elH, 0.08055);
  Acrylic->AddElement(elO, 0.31961);
```

Figure 4.1: The fragment of the simulation code. This part declares the elements and materials. a is the atomic weight, z is the atomic number.

Physics List class

The physics process and the particles must be defined in this class. In addition, the range of cut-off parameter should also be defined in this section. GEANT4 provides many physics processes, which describe how particles interact with materials, such as electromagnetic, hadronic, transportation, decay, optical and parameterisation. It also provides data of many particles, such as electrons, protons, gammas and so on. They are organized into six categories, lepton, meson, baryon, boson,

29

```
G4double innerRadiusOfTheTube= 0.*cm;
G4double outerRadiusOfTheTube= 5.08*cm;
G4double hightOfTheTube= 5.08*cm;
G4double startAngleOfTheTube= 0.*deg;
G4double spanningAngleOfTheTube= 360.*deg;

G4RotationMatrix *rot= new G4RotationMatrix;
rot->rotateY(90*deg);

G4Tubs* NE213detector_tube = new G4Tubs("NE213detector_tube",
                                        innerRadiusOfTheTube,
                                        outerRadiusOfTheTube,
                                        hightOfTheTube,
                                        startAngleOfTheTube,
                                        spanningAngleOfTheTube);
NE213detector_log = new G4LogicalVolume(NE213detector_tube, NE213,"detector_log",0,0,0);
NE213detector_phys = new G4PVPlacement(rot,                    //  rotation set
                                       G4ThreeVector(0,0,0),   //  translation position
                                       NE213detector_log,      //  its logical volume
                                       "detector",             //  its name
                                       experimentalHall_log,   //  its mother volume
                                       false,                  //  no boolean operations
                                       0);                     //  its copy number
```

Figure 4.2: The fragment of the simulation code. This part describes the geometry of NE213 detector. This creates a cylinder of radius 5.08 cm and length 10.16 cm. The cylindrical solid is filled with NE213 materials.

shortlived, and ion. Fig. 4.3 and Fig. 4.4 show the fragment code to define the particles and physical process.

```
void NeuCapPhysicsList::ConstructParticle()
{
  // Construct all particles which you want to use.
  ConstructBosons();
  ConstructLeptons();
  ConstructMesons();
  ConstructBaryons();
  ConstructAllIons();
  ConstructAllShortLiveds();
}

void NeuCapPhysicsList::ConstructBosons()
{
  // bosons
  G4BosonConstructor pConstructor;
  pConstructor.ConstructParticle();
}
```

Figure 4.3: The fragment of the simulation code. This part is defining the particles.

```
void NeuCapPhysicsList::ConstructProcess()
{
  AddTransportation();  // Define transportation process
  AddParameterisation();// Define fast simulation manager process
  ConstructGeneral();   // Define decay process
  ConstructEM();        // Define electromagnetic process
  ConstructHad();       // Define hadronic process
  ConstructIon();       // Define process for ions
  ConstructOp();        // Define optical process
}
```

Figure 4.4: The fragment of the simulation code. This part is defining the physics process.

Primary Generator Action class

This section is for user to define the details of initial particle, that is, setting the particle gun. User has to set the particle for particle gun and its energy, direction. Fig. 4.5 shows the fragment code for defining the incident particle and its direction.

31

```
theta2=float(16.83*rand()/(RAND_MAX+1.0))+180;    //for NE213 25.765 cm
phi2=float(360.0*rand()/(RAND_MAX+1.0));
vz=sin(theta2*PI/180)*cos(phi2*PI/180);
vy=sin(theta2*PI/180)*sin(phi2*PI/180);
vx=cos(theta2*PI/180);

std::string path=getenv("G4WORKDIR");
path +="/neutron_capture/";
std::string spectrumFile=path+"Pu238C0.root";
specfile=TFile::Open(spectrumFile.c_str());
hEmitted=(TH1F*)specfile->Get("hEmittedNeutronEnergy");
double randomEnergy=(hEmitted->GetRandom())*MeV;

G4ParticleTable* particleTable = G4ParticleTable::GetParticleTable();
G4ParticleDefinition* particle = particleTable->FindParticle("neutron");
particleGun->SetParticleDefinition(particle);
particleGun->SetParticleMomentumDirection(G4ThreeVector(vx,vy,vz));
particleGun->SetParticleEnergy(randomEnergy);
```

Figure 4.5: The fragment of the simulation code. This part describes the geometry of NE213 detector.

4.2 Experimantal Simulation

We use GEANT4 to simulate the neutron detection experiments with NE213 organic liquid scintillator and ^3He proportional tube.

The geometry of experiment target, which is a NE213 organic liquid scintillator and ^3He proportional tube, are shown in Fig. 4.6 and Fig. 4.7. The detectors are cylinders and the figures are the cross-section view. We assume the NE213 detector consist of three parts, liquid scintillator, acrylic, and aluminum shell; the ^3He proportional tube consist of an aluminum shell and ^3He gas. The details of the experimental condition are shown in Table 4.1.

We also consider that some of neutrons scattered from the wall may have a chance to pass through the detector. Therefore, we add the wall into the simulation environment. We assume the material of the wall is concrete and the dimension is $3\times5\times7$ m. The detectors are set in the center and the neutron source is set in front of the detector, as shown in Fig. 4.8.
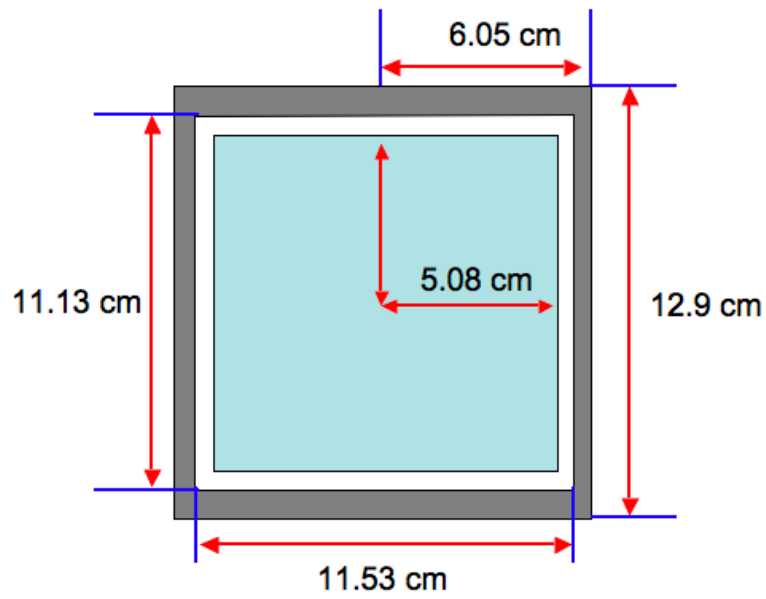
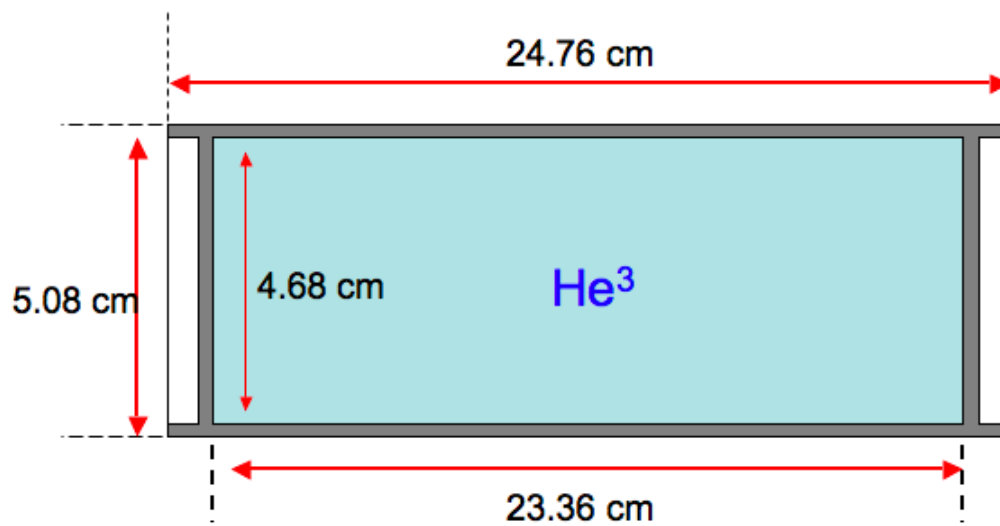Figure 4.6: Liquid scintilator Detector geometry in GEANT4.

Figure 4.7: ^3He Detector geometry in GEANT4.

Materials	Density	Elements/Ratio	Pressure	Temperature
Air	1.29 mg/cm^3	N:O / 0.7:0.3	1 atm	293.15 K
Helium-3	0.0005 mg/cm^3		4 atm	
NE213	0.874 g/cm^3	H:C / 0.54812:0.45188		
Acrylic	1.18 g/cm^3	C:H:O / 0.59984:0.08055:0.31961		
Concrete	2.4 g/cm^3	H,O,Na,Mg,Al,Si,K,Ca,Fe		

Table 4.1: The simulation parameter details.
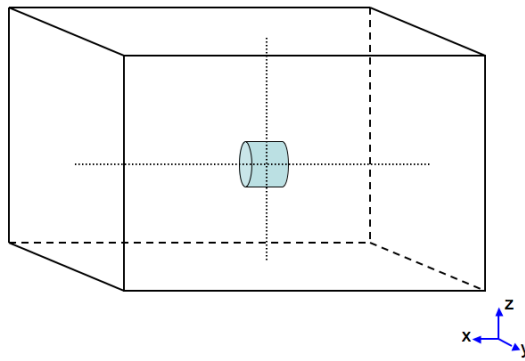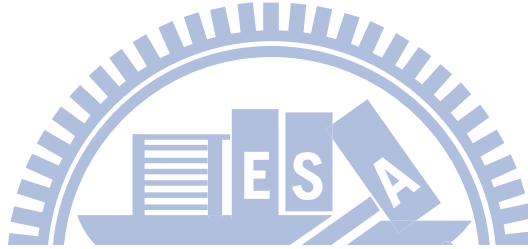
Figure 4.8: The detector is put in the center of the "room". The length of x direction is 5 meter, y is 7 m, and z is 3 m.

With the GEANT4 program, we have neutron incident on the target with different energies. Actually, we fed the original source spectrum that is also a simulation result, as shown in Fig. 4.9, into the particle gun. The simulation was done by J. Liu [14]. He simulated the two steps process of Pu^{238} and C^{13}. The x-axis is energy in MeV and the y-axis is proportional to the probability. During the simulation, the GEANT4 program selects the random energy according to this distribution.
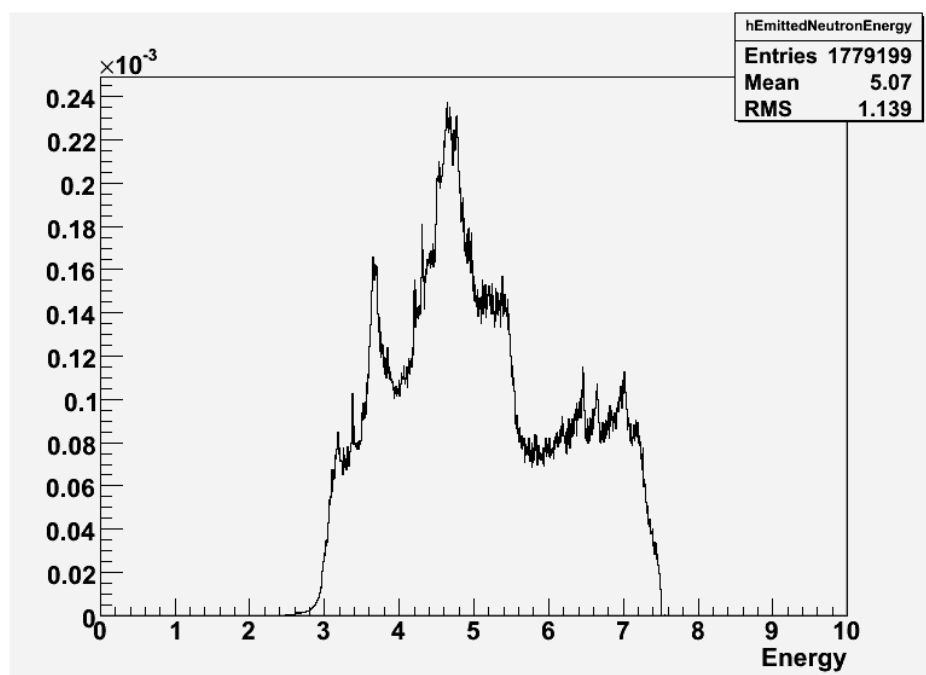

Figure 4.9: The spectrum of the source $Pu^{238}C^{13}$. It is a simulation result, done by J. Liu [14].

The direction of radiation particles is isotropic. For considering the simulation efficiency, we just let the particle direction random in the solid angle with respect to the detector surface. The distance between the particle gun and the detector surface is 20 cm. For NE213 detector, the radius of detector shell is 6.05 cm; for ^3He proportional tube, the radius of detector shell is 2.54 cm. Hence θ is about 16.83 degrees and 4.56 degrees, respectively.
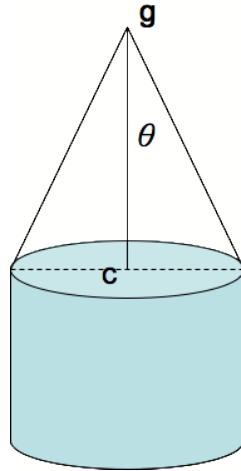
Figure 4.10: The particle gun is at point g, and point c is the center of circle. $\overline{gc} = 20cm$. θ is 16.83^o for NE213 detector, and it is 4.56^o for ^3He proportional tube.

For the NE213 detecting system, we did not consider the efficiency of scintillation. When neutron elastic process takes place in the detector and produces the recoil particles, we record the information of particles. For ^3He proportional tube, when neutron interacts with ^3He and then produces a triton and proton, we record their information. Finally, we analyze these data and plot histograms.

Chapter 5

# The Measurement of Monoenergic Neutron Source

5.1   Neutron Production

To check the normalization of GEANT4 simulation, we detect the monoenergetic neutron. The monoenergetic neutron can be produced by (p,n) and (d,n) reactions with accelerated proton and deuteron. The neutron energy can be calculated according to

$$
E_n = E\frac{m_G m_n}{(m_n + m_r)^2}\left\{2\cos^2\vartheta + \frac{m_r(m_n + m_r)}{m_G m_n}\left[\frac{Q}{E} + \left(1 - \frac{m_G}{m_r}\right)\right]\right.
$$
$$
\left. \pm\, 2\cos\vartheta\sqrt{\cos^2\vartheta + \frac{m_r(m_n + m_r)}{m_G m_n}\left[\frac{Q}{E} + \left(1 - \frac{m_G}{m_r}\right)\right]}\right\}, \quad (5.1)
$$

where E_n is neutron energy, m_n is neutron mass, E is energy of the projectile, m_G is the mass of projectile, m_r is the mass of residual nuclei, Q is the Q-value, and ϑ is the angle of neutron emssion with respect to direction of the projectile.

(d, n) reaction

$$
{}_z^A X + d \rightarrow {}_{z+1}^{A+1} X + n + Q
$$

37
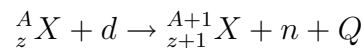
For most neutron production from the accelerator reaction, deuteron impacting on target through (d, n) reaction is the most popular method. There are two channels of (d, n) reaction. First, deuteron can be captured by a nucleus and become an excited compound nucleus. A nucleus then releases a neutron. The second channel is deuteron fission. The widely used (d, n) reaction are $T(d, n)$, $D(d, n)$, $^{12}C(d, n)$, $^{9}Be(d, n)$, and $^{7}Li(d, n)$...etc.[†] The first three reactions are mainly generated by the van de Graff accelerator.

The neutron energy can be estimated by Eq. (5.1). Roughly, the neutron energy produced from $D(d, n)$ reaction is between 2 and 10 MeV; while it is between 12 and 20 MeV in $T(d, n)$ reaction.

In this experiment, we produced neutron by (p, n) reaction.

(p, n) reaction

$$^{A}_{z}X + p \rightarrow ^{A}_{z+1}X + n + Q$$
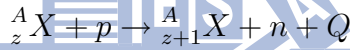
Proton impacts on the target nucleus $^{A}_{Z}X$ and a neutron is produced in the final state. The final nucleus is the isotope of the original nucleus. This process is referred to as (p, n) reaction. This reaction is also widely used as the neutron source in van de Graff accelerator. A monoenergetic neutron source can be produced through this reaction.

[†]The reaction equations:

$$T + d \rightarrow n + {}^{4}He \qquad\qquad Q = 17.588 \text{ MeV} \qquad\qquad (5.2)$$

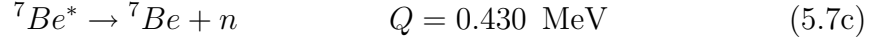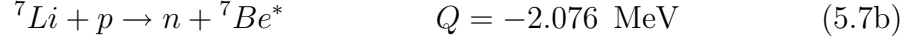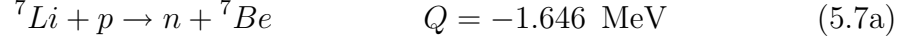$$D + d \rightarrow n + {}^{3}He \qquad\qquad Q = 3.28 \text{ MeV} \qquad\qquad (5.3)$$

$$^{12}C + d \rightarrow n + {}^{13}N \qquad\qquad Q = 0.281 \text{ MeV} \qquad\qquad (5.4)$$

$$^{9}Be + d \rightarrow n + {}^{10}Be \qquad\qquad Q = 4.362 \text{ MeV} \qquad\qquad (5.5)$$

$$^{7}Li + d \rightarrow n + {}^{8}Be \qquad\qquad Q = 15.028 \text{ MeV} \qquad\qquad (5.6a)$$

$$^{7}Li + d \rightarrow n + 2{}^{4}He \qquad\qquad Q = 15.122 \text{ MeV} \qquad\qquad (5.6b)$$

$^7Li(p,n)^7Be$ **reaction** The most frequently used (p,n) reaction for producing the monoenergetic neutrons is

$$^7Li + p \rightarrow n + {}^7Be \qquad\qquad Q = -1.646 \text{ MeV} \qquad\qquad (5.7\text{a})$$

$$^7Li + p \rightarrow n + {}^7Be^* \qquad\qquad Q = -2.076 \text{ MeV} \qquad\qquad (5.7\text{b})$$

$$^7Be^* \rightarrow {}^7Be + n \qquad\qquad Q = 0.430 \text{ MeV} \qquad\qquad (5.7\text{c})$$

The proton threshold energy for this reaction is 1.881 MeV. For this proton energry, the neutron energy is 0.03 MeV (forward direction). According to the Eq. (5.1), the neutron energy decreases continuously as ϑ increases. The neutron yield decreases with the neutron angle with respect to the proton direction.

$^3H(p,n)^3He$ **reaction** Since ^3He does not have excited states, this reaction is usually applied to produce neutrons.

$$^3H + p \rightarrow n + {}^3He \qquad\qquad Q = 0.764 \text{ MeV} \qquad\qquad (5.8)$$
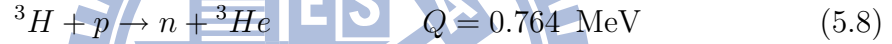
The threshold energy of this process is 1.019 MeV, and the corresponding neutron energy is 63.7 KeV. Gas targets is usually used for this process.

5.2 Experiment Setup

The protons produced by accelerator impacting on the target can generate the monoenergetic neutrons. The reactions are mentioned in the last section. Since these neutrons are monoenergetic, they can be used to calibrate the detection systems or the results of simulation.

5.2.1 Accelerator

The accelerator in the National Tsing Hua University is tandem accelerator. The tandem accelerator is a type of electrostatic accelerators, which is shown in Fig. 5.1.

The model of this accelerator is the Model 9SDH-II Tandem Accelerator. It was designed by National Electrostatics Corporation, USA.

The largest terminal voltage of the accelerator is 3 MeV, it includes the tandem Van de Graaff accelerator, the source of negative ion by cesium sputtering, SNICS, the high precise analyzing magnet, and the switching magnet. The negative ions are accelerated and arrive to the positive high voltage electrode by the attractive force. While they pass through the gas stripping canal, they become positive ions. The positive ions are then accelerated again by the repulsive force.

To obtain the 4 MeV proton, the ion source we used was TiH_2 and the terminal voltage was set at 1.587 MeV.
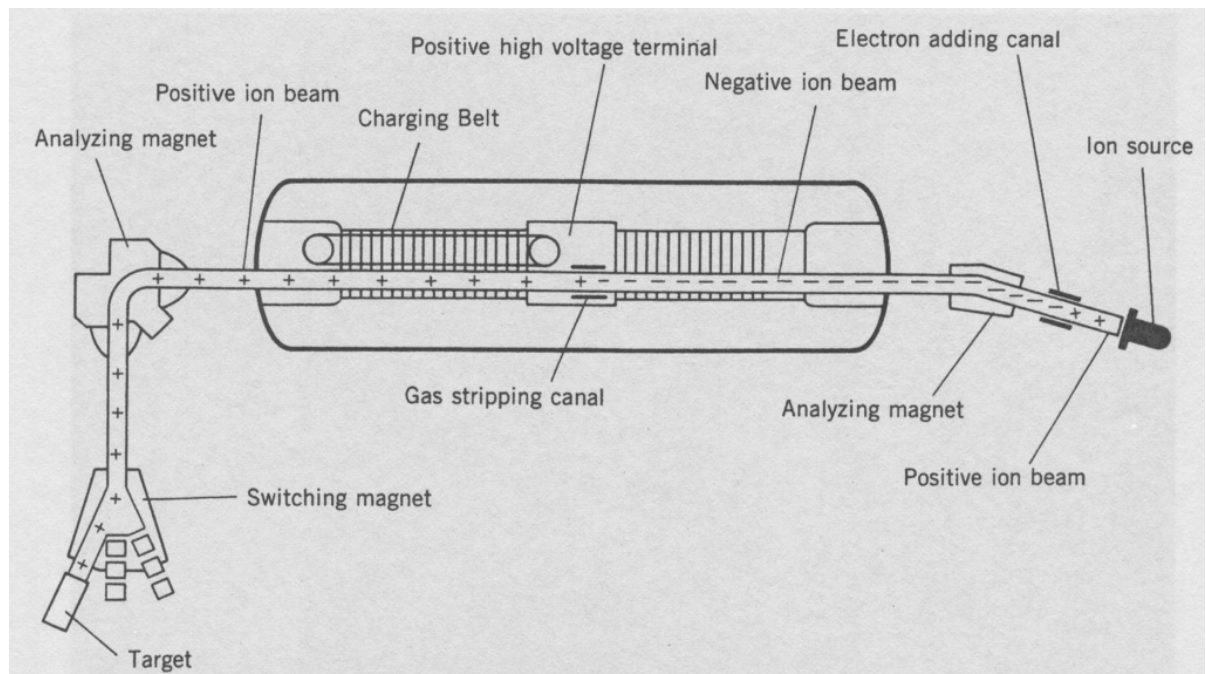
Figure 5.1: The tandem accelerator.

5.2.2 Target

We used silicon chip as a backing. After cleaning the backing chip, we apply the evaporation method for plating TLD-700, LiF, on the backing chip. Actually, the

TLD-700 also contains Mg and Ti. Fig. 5.2 shows the evaporation instrument. The thickness of the TLD-700 on the target is about 200 nm. The target is fixed on the end of the bean line, Fig. 5.3.

Figure 5.2: The evaporation instrument.

5.2.3 Detector Setup

As mentioned before, the neutron yield decreases as the angle increases. So, we placed detectors close to the zero-angle position. The angle between the NE213 detector and ^3He tube is about 30°. We set a restrictor in front of the target, actually, there is a ceramic tube between the restrictor and the target. The restrictor has an opening with a 4 mm diameter. When the proton passes through the opening of the restrictor and impacts on the target, there are positive charges accumulating on the end of the valve that is made of steel. We then used a cable connecting with a current integrator, the Model 439 Digital Current Integrator, so that we can estimate the number of protons which impact on the target.
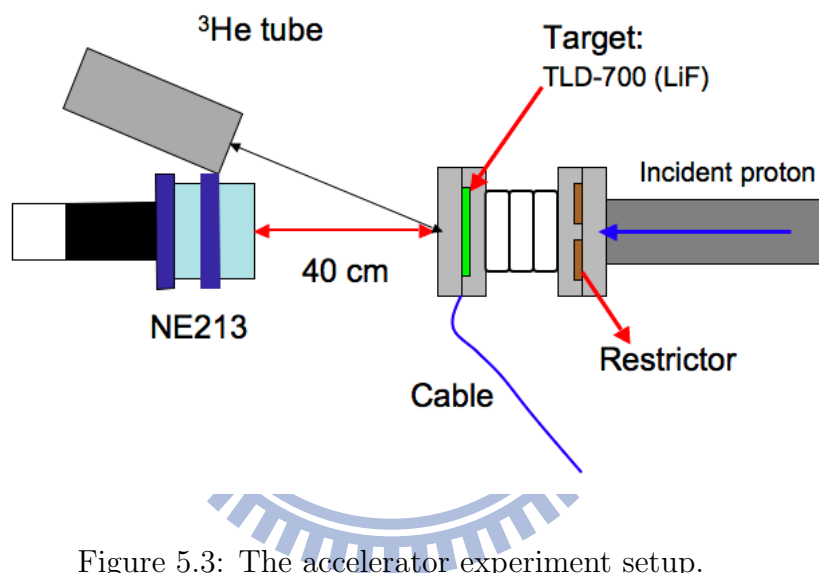
Figure 5.3: The accelerator experiment setup.
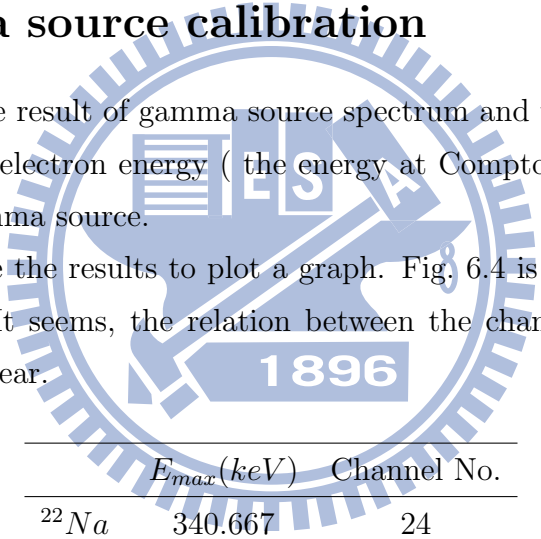
Chapter 6

Results and Discussion

6.1 Gamma source calibration

The following are the result of gamma source spectrum and their differentiations. Table 6.1 shows the electron energy (the energy at Compton edge) and channel number for each gamma source.

Therefore, we use the results to plot a graph. Fig. 6.4 is the result of gamma source calibration. It seems, the relation between the channel number and the electron energy is linear.

	$E_{max}(keV)$	Channel No.
^{22}Na	340.667	24
	1061.71	67
^{137}Cs	477.336	31
^{54}Mn	639.202	41

Table 6.1: The result of gamma calibration.
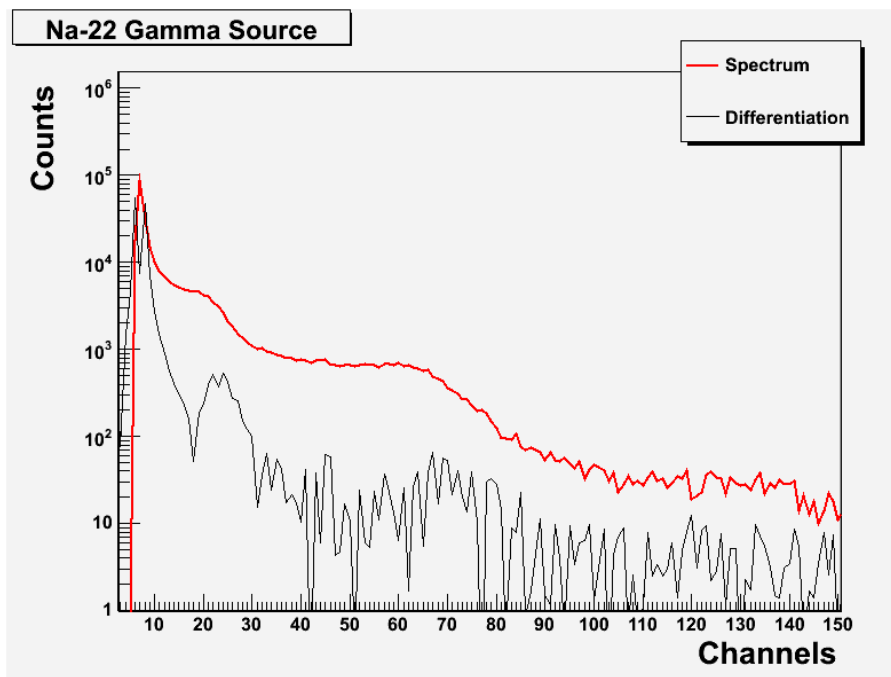
Figure 6.1: Na-22 source spectrum. There are two Compton edge at channel 24 and channel 67.
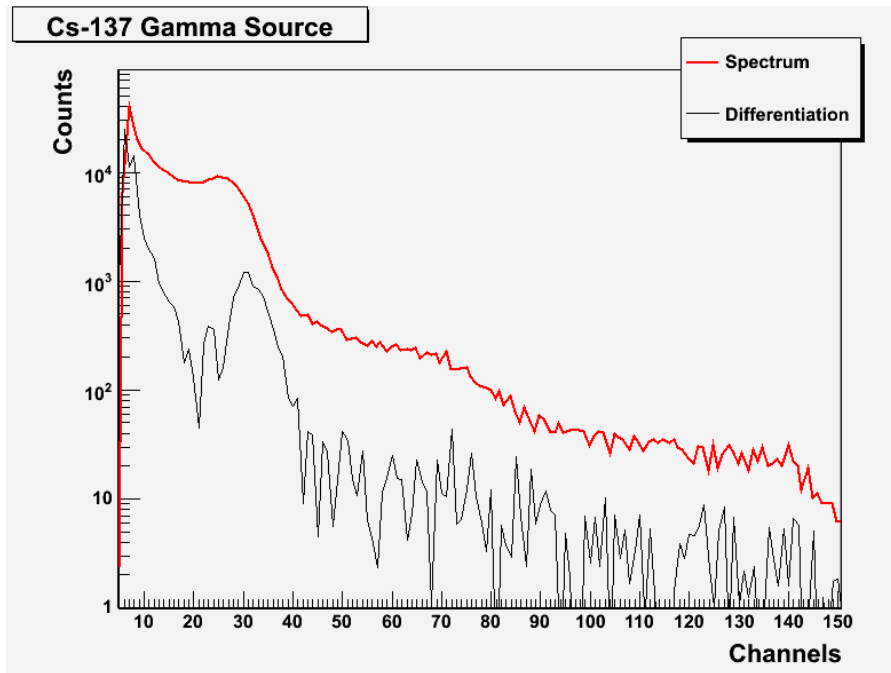
Figure 6.2: Cs-137 source spectrum. There is a Compton edge at channel 31.
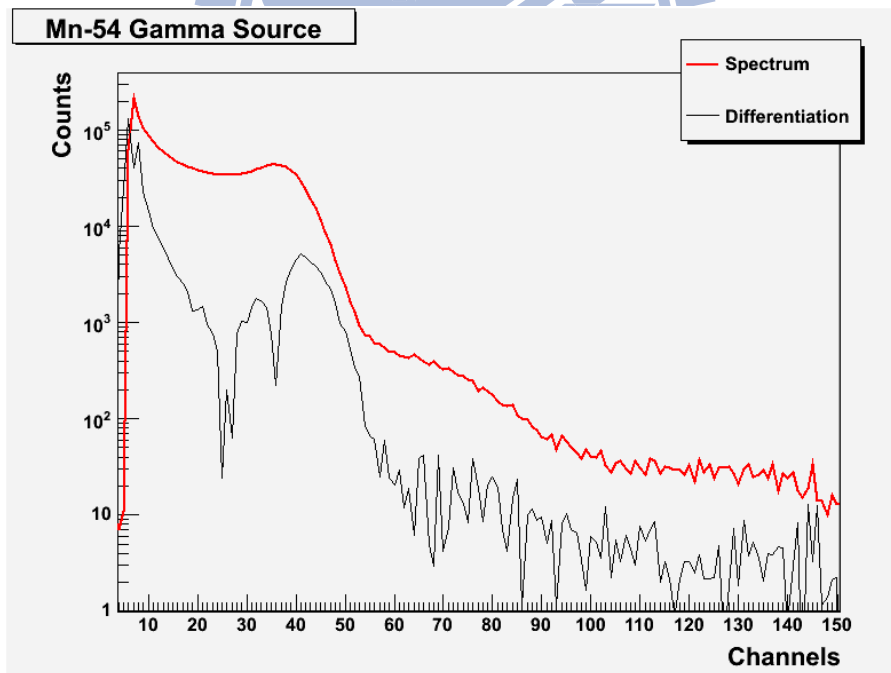
Figure 6.3: Mn-54 source spectrum. There is a Compton edge at channel 41.
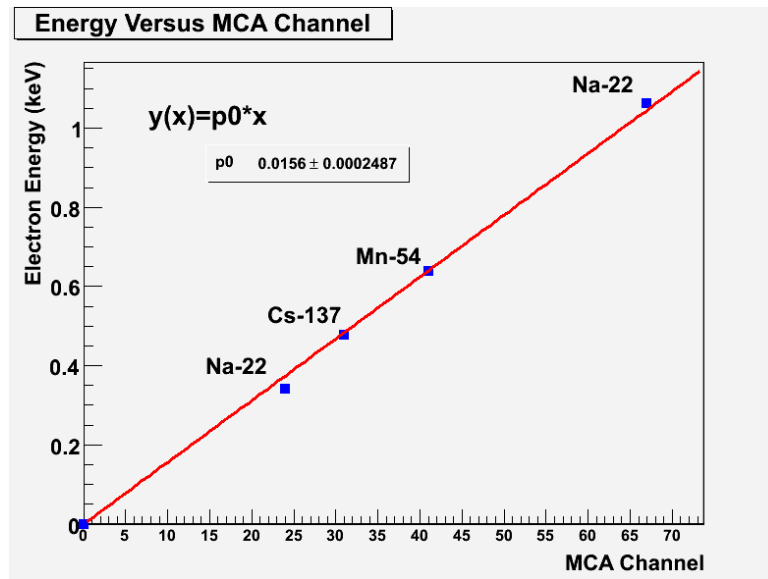
Figure 6.4: The Electron Energy Versus MCA Channel.

6.2 Gamma and neutron signal pulse shape discrimination

Fig. 6.5 shows the time constant spectrum of gamma and neutron signal of the Pu^{238}-C^{13} source; Fig. 6.6 shows the result of the monoenergic source. The peaks that at the range of channel 30 to channel 40 are the gamma signals, and those at the range of channel 160 to channel 190 are neutron signal.

Therefore, to do the signal coincidence, we selected the time window between channel 160 and channel 190.
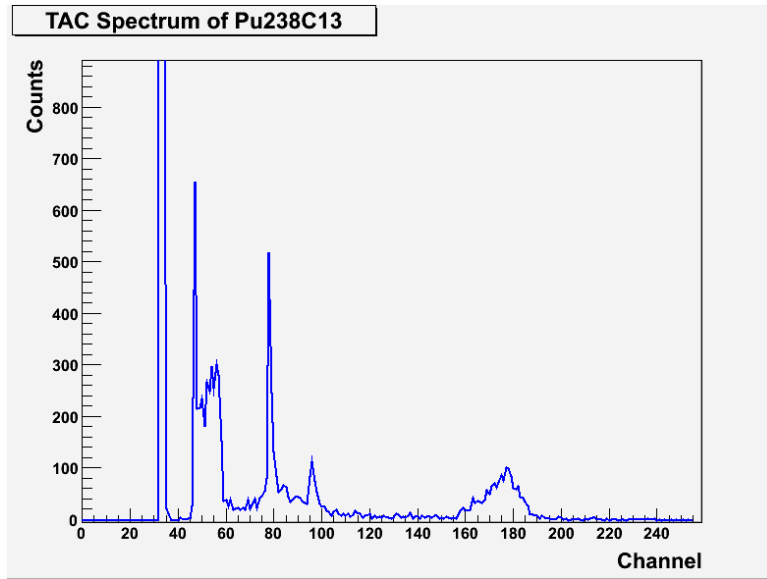
Figure 6.5: The time constant spectrum of Pu^{238}-C^{13} source.
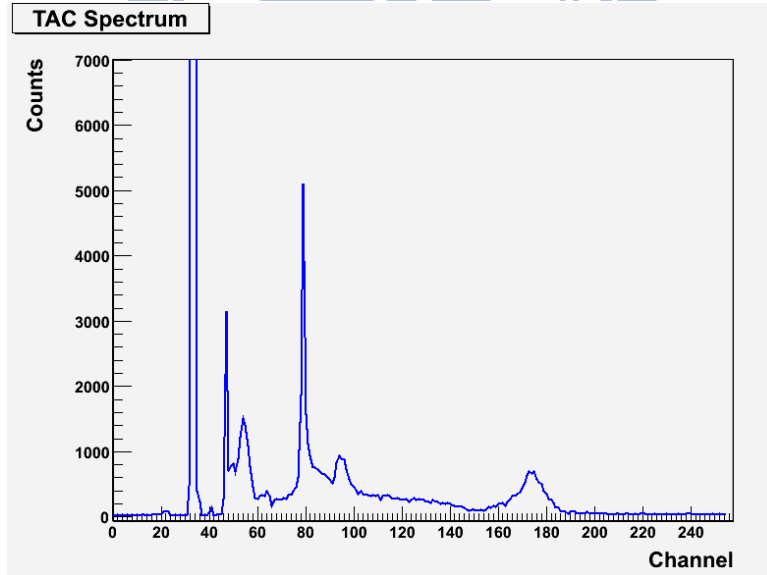
Figure 6.6: The time constant spectrum of monoenergic neutron source.

47

6.3 The result of neutron source measurement and its comparison to the simulation

6.3.1 The Pu^{238}-C^{13} source spectra

The results of the NE213 detector

a) The result of measurement The measured spectrum is shown in Fig. 6.7. However, this is not the real neutron spectrum. As mentioned before, neutrons are only indirectly detected, and the measurement of neutron energies is through the proton recoil. The result in Fig. 6.7 is the proton energy spectrum.
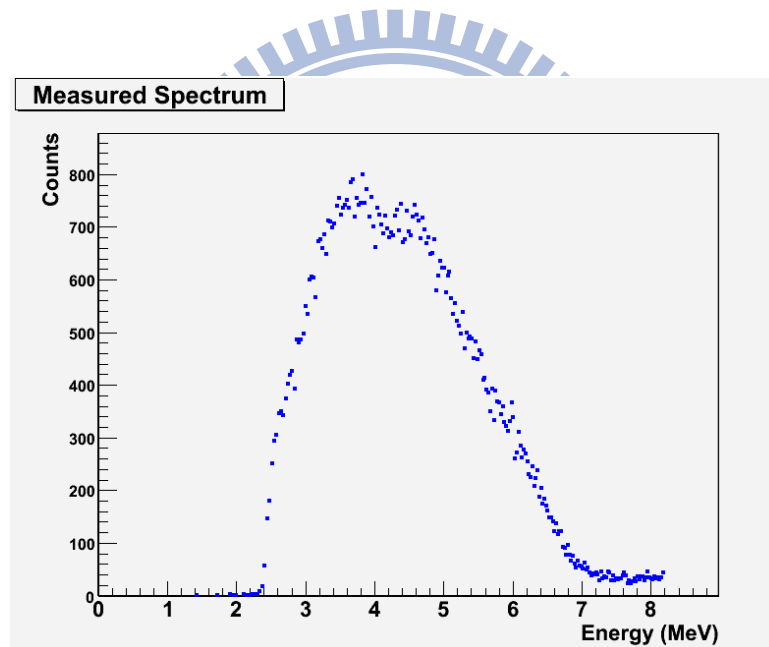
Figure 6.7: Measured spectrum from NE213 detector. The channels range of the time constant spectrum is from the channel 160 to the channel 190.

b) The result of simulation   We use GEANT4 toolkit to perform the simulation. Fig. 6.8 shows the result of NE213 detector simulation. This result includes up to the triple recoil of the proton in the NE213 detector.
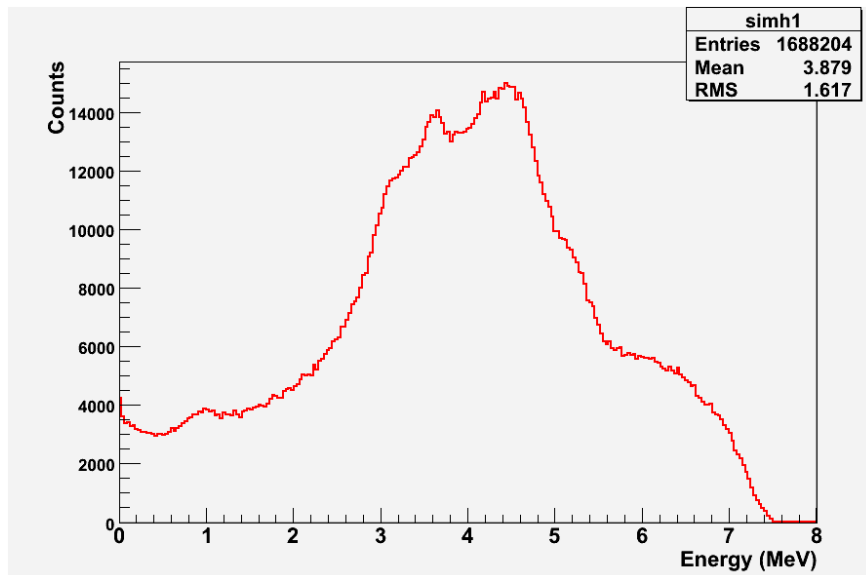

Figure 6.8: Neutron detection simulation for NE213 detector.

c) Comparison   Fig. 6.9 shows the comparison of measurement and simulation results. The normalizing range is between 2.5 MeV and 8 MeV. As one can see, for the NE213 detection system, there is a cutoff at about 2.5 MeV. This is the energy threshold for our measurement.
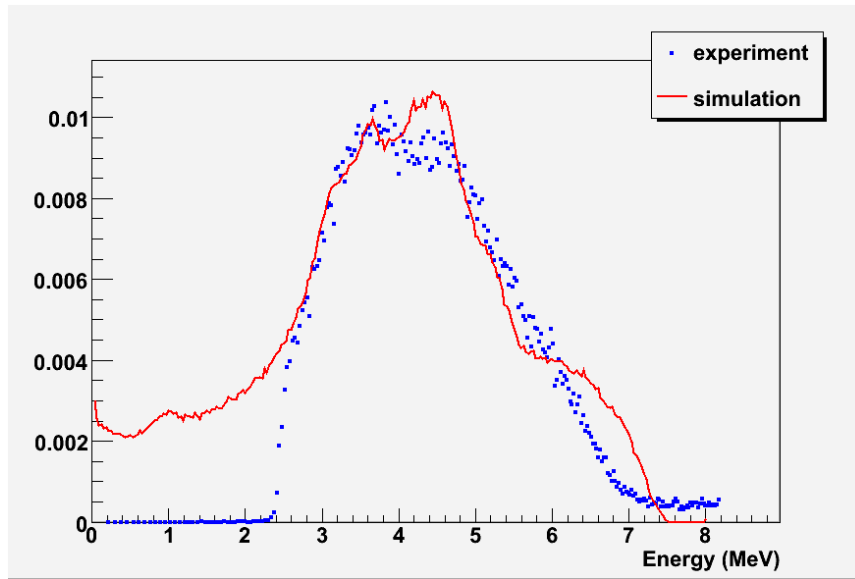
Figure 6.9: The comparison of simulation and measurement for the proton recoil spectrum. The area under the curve between 2.5 MeV and 7 MeV is used to set the normalization.

The result of ^3He proportional tube

a) The result of measurement The measured spectrum of Helium-3 proportional detector is shown in Fig. 6.10. The peak in the spectrum is the thermal neutron reaction energy which is 0.764 keV. We divide 0.764 keV by the channel number which is at the peak location and we obtain the energy per channel. Therefore we obtain the energy scale for neutron.[†]

b) The result of simulation Fig. 6.11 shows the result of ^3He proportional tube simulation.

[†]The events lower than 0 MeV are the wall effect of the detector. They are the energies of the proton or triton. More information about wall effect is given in Ref. [5]
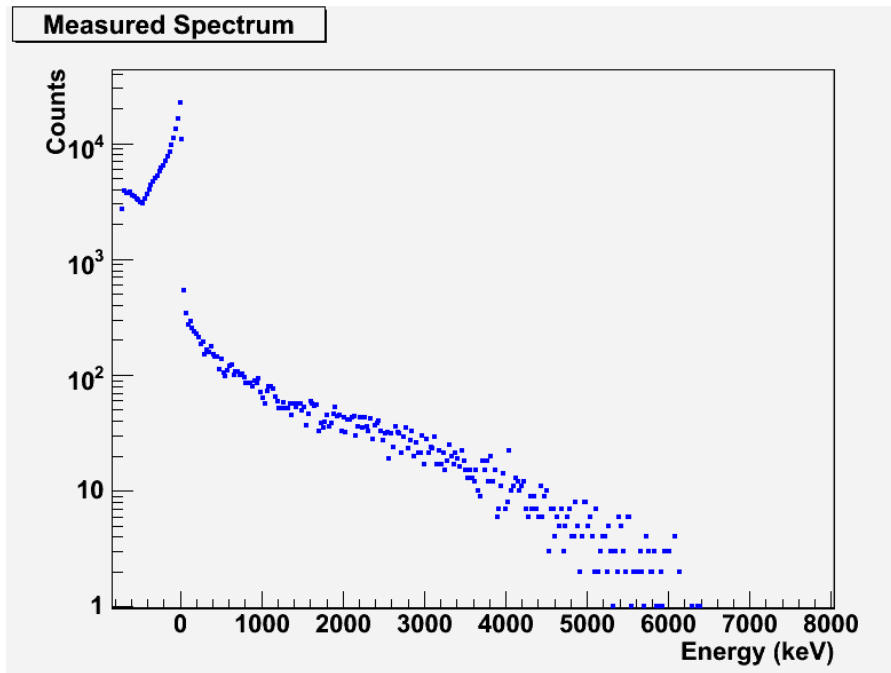
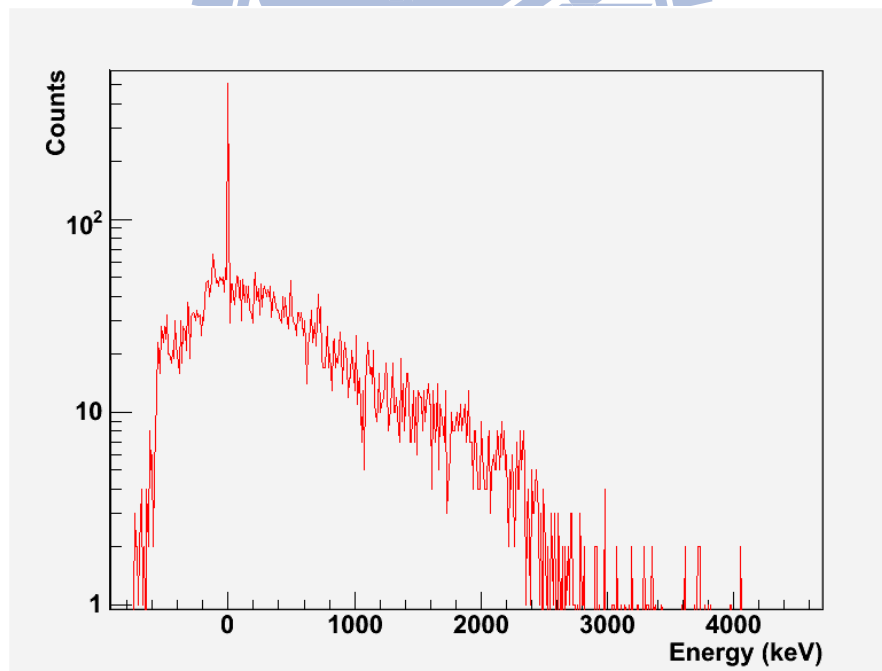Figure 6.10: Measured spectrum by Helium-3 detector.

Figure 6.11: Neutron detection simulation for He^3 proportional tube.

51

c) Comparison   Fig. 6.12 shows the comparison between measurements and simulations. We use the maximum value of the results to normalize the data. It is easy to see that the simulation is greater than measurement when the energy is more than 0 MeV. However, for events due to the wall effect, the experiment is more sensitive than the simulation.
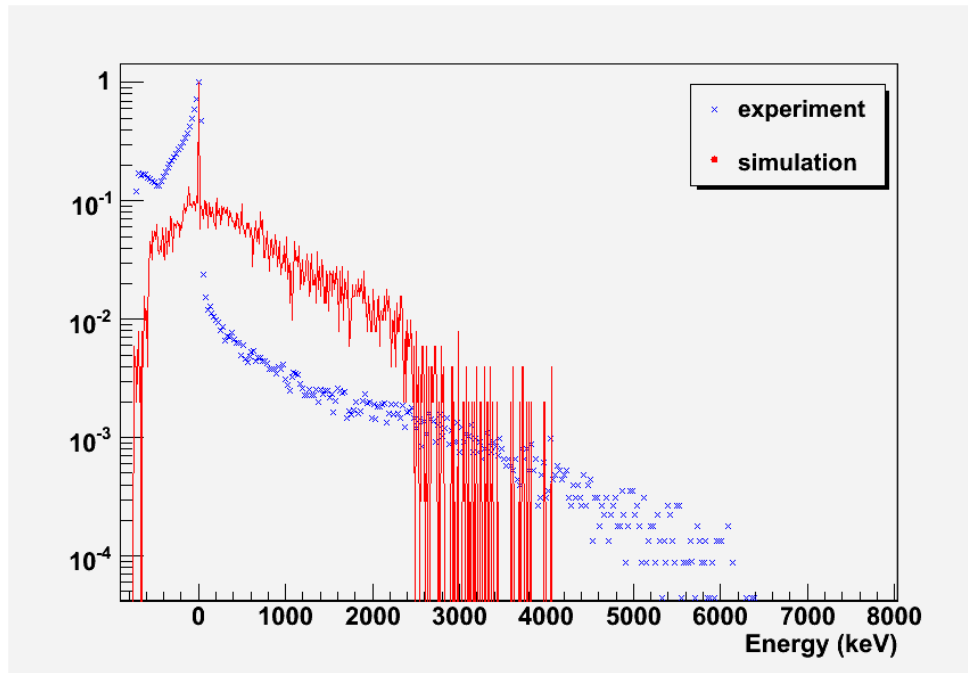

Figure 6.12: The normalized result for the simulation and experiment of the ^3He proportional tube.

6.3.2 The monoenergic neutron source spectra

The results of the NE213 detector

a) The result of measurement Fig. 6.13 shows the recoil proton spectrum resulted from the monoenergic neutron source generated by Van de Graff accelerator.
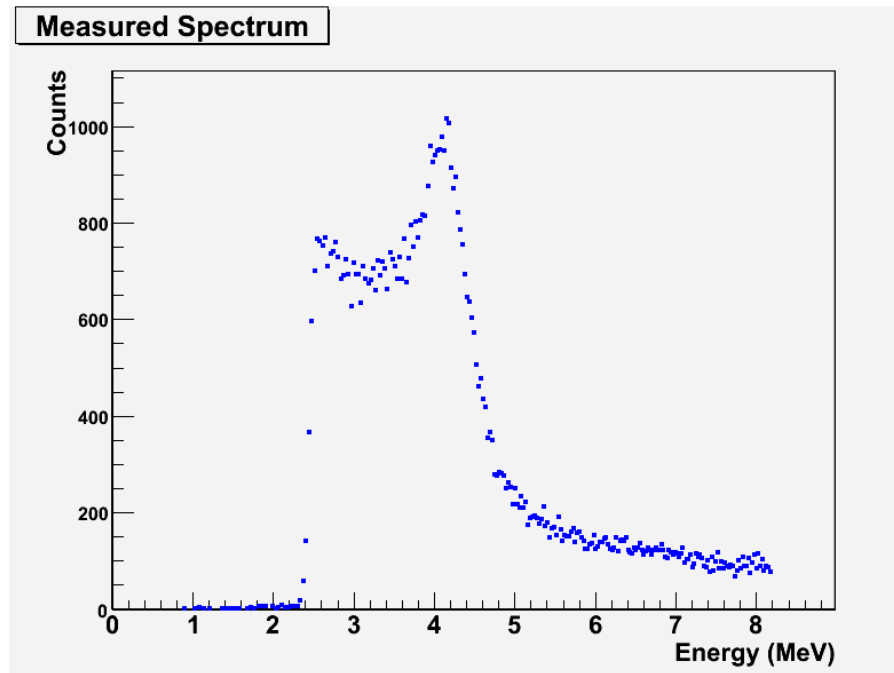

Figure 6.13: The measured spectrum by NE213 detector. The channels range of the time constant spectrum are from the channel 160 to the channel 190.

b) The result of simulation We are do not simulate the process, $^7Li(p,n)^7Be$. However, since neutron is known to be monoenergetic, we set the neutron kinetic energy as 2.7 MeV.
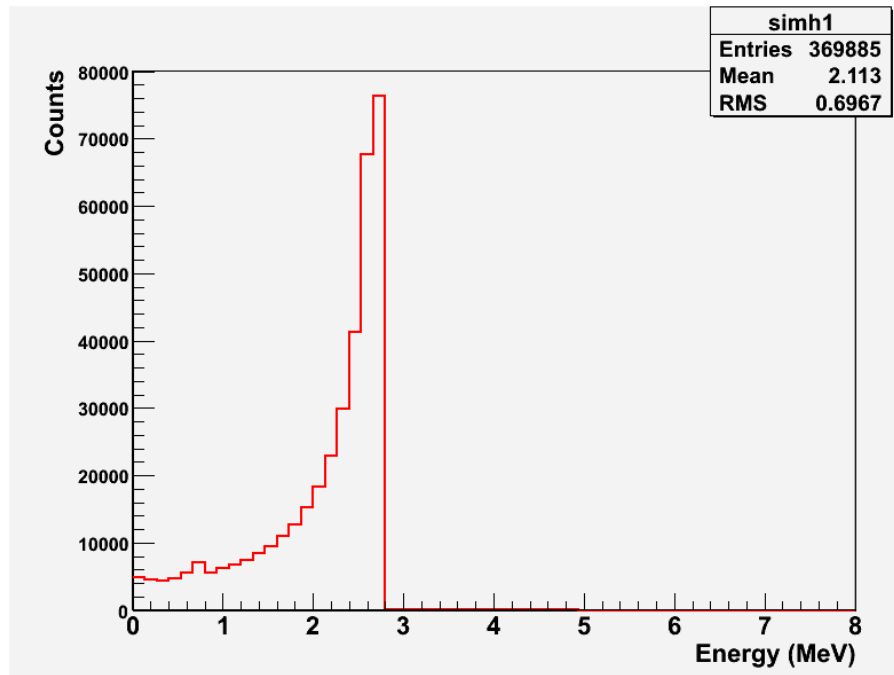

Figure 6.14: The simulated spectrum in NE213 detector resulted from the monoenergic neutron source.

Obviously, these two results are hard to compare, since the lower limit of the detecting system is around 2.5 MeV; while the maximum value for recoil proton energy is 2.7 MeV. We do not know the trend less than 2.5 MeV in the measured spectrum.

The result of ^3He proportional tube

a) The result of measurement   Fig. 6.15 shows the neutron spectrum measured by ^3He proportional tube.
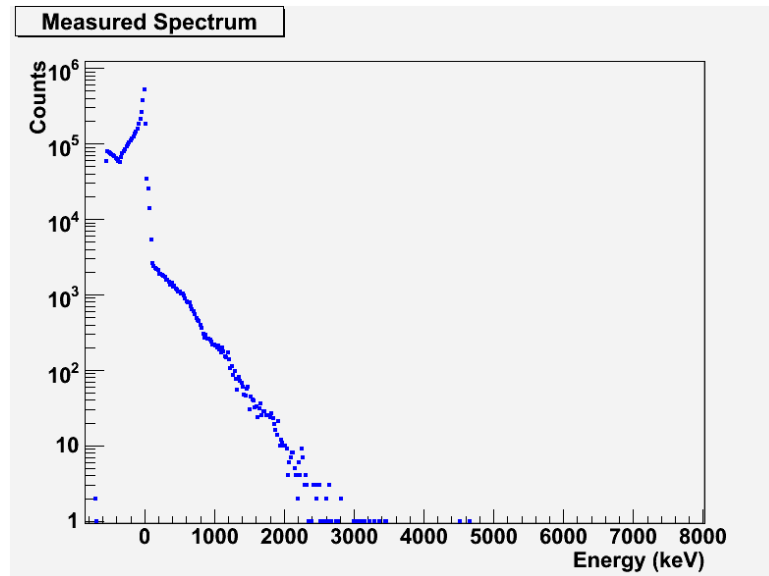

Figure 6.15: The neutron spectrum measured by ^3He proportional tube.

b) The result of simulation   Fig. 6.16 shows the simulated neutron spectrum in ^3He proportional tube.

c) Comparison   Fig. 6.17 shows the comparison of normalized results. Similar to the previous case, the experimental result is more sensitive at the wall effect and the simulation result is more sensitive at energies larger than 0 MeV.
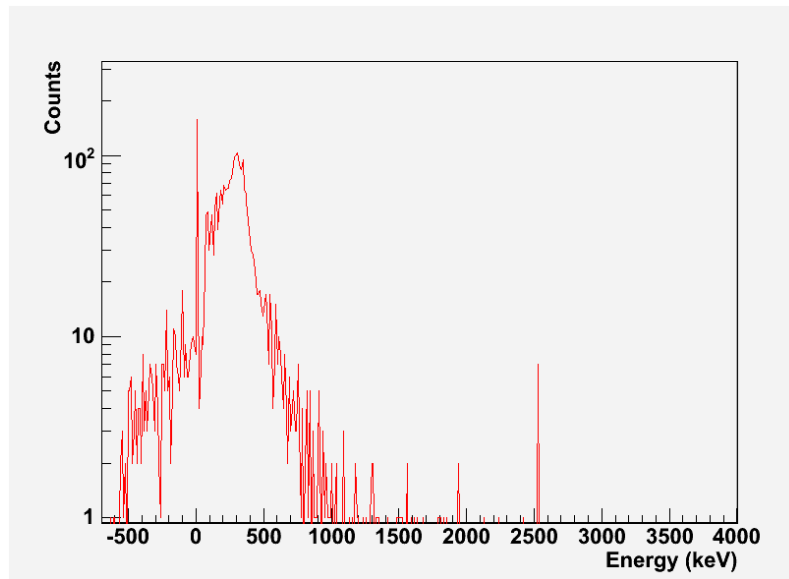
Figure 6.16: The simulated neutron spectrum in ^3He proportional tube.

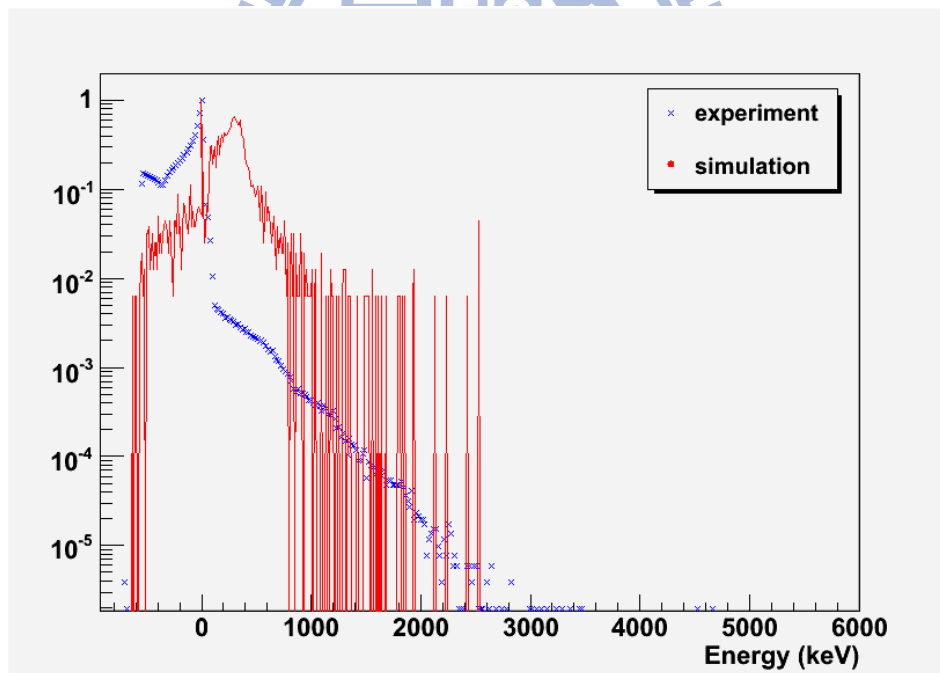Figure 6.17: The normalized result of the simulation and experiment of the ^3He proportional tube.

Chapter 7

Conclusion

The result of neutron energy measurement by NE213 detecting system is consistent with the result by simulation except for the energy lower than 2.5 MeV. The ^3He proportional tube detector is however not suitable for measuring fast neutrons.

To produce monoenergic neutron source, we have protons with a kinetic energy 4.4 MeV impact on the LiF target, the neutrons were generated with the maximum of the kinetic energy 2.73 MeV at the zero degree position which can be estimated by Eq. 5.1. It is unreasonable to observe neutron energy greater than 2.73 MeV. However, there always exists a peak at 4 MeV in the result of NE213 detector, as shown by Fig. 6.13. We also see the same peak at different time constant ranges, as shown by Fig. 7.1 and Fig. 7.2. It is hard to explain where does those events come from. So we suggest another measurement of this effect with different neutron detection method. Furthermore, for producing the monoenergic neutron, we can also use the other processes, such (d, n) reaction. The neutron energy from these processes is larger than (p, n) reaction. It might be more preferred for the NE213 detecting system.
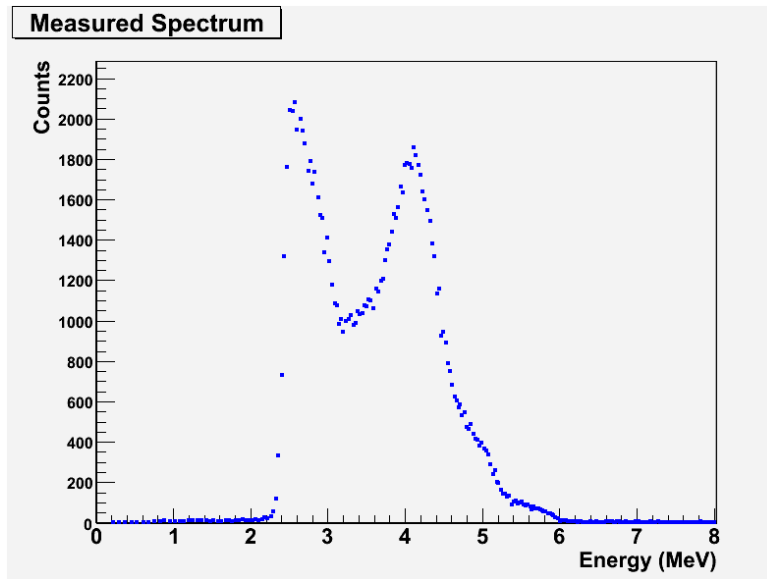
Figure 7.1: The measured spectrum by NE213 detector. The channels range of the time constant spectrum are from the channel 46 to the channel 60.
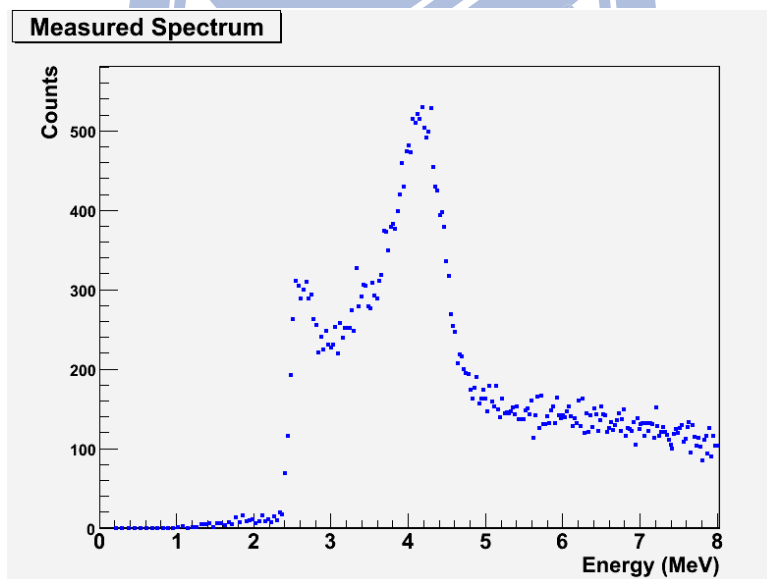

Figure 7.2: The measured spectrum by NE213 detector. The channels range of the time constant spectrum are from the channel 75 to the channel 86.

Bibliography

[1] X. Guo *et al.* [Daya Bay Collaboration], arXiv:hep-ex/0701029.

[2] J. R. Chen *et al.*, Nucl. Sci. J. **19(2)**, 81 (1982).

[3] M. Karlsson, Master thesis, Department of Nuclear Physics in Lund, University of Lund, Sweden (1997).

[4] Y. S. Yeh *et al.*, Nuclear Science Symposium Conference Record, IEEE, vol. **3**, 2016(2007).

[5] G. F. Knoll,"Radiation Detection and Measurement", 3rd Edition, Wiley (2000).

[6] W. R. Leo,"Techniques for Nuclear and Particle Physics Experiments", 2rd Edition, Springer-Verlag (1994).

[7] L. M. Bollinger and G. E. Thomas, Rev. Sci. Instrum. **32**, 1044(1961).

[8] N. Tsoulfanidis,"Measurement and Detection of Radiation", 2nd Edition, Taylor&Francis (1995).

[9] J. B. Birks,"The Theory and Practice of Scintillation Counting", Pergamon Press, Oxford (1964).

[10] H. Klein and S. Neumann, Nucl. Instrum. Methods **A476**, 132-142(2002).

[11] R. D. Evans, "The Atomic Nucleus", McGraw-Hill (1955).

[12] K. H. Beckurts and K. Wirtz, "Neutron Physics", Springer (1964).

[13] http://www.geant4.org/geant4/

[14] J. Liu, privately consult.

[15] Kenneth S. Krane, "Introductory Nuclear Physics", John Wiley & Sons (1988).